CHAPTER 1

INTRODUCTION

1.1 General

In the world of today, there is a growing demand for high performance machinery components such as gear, owing to their robust qualities – high strength; corrosion and wear resistant; etc. To meet the demand, application of several surface engineering techniques are very much indispensable to improve and enhance the properties of the material used. Chemical Vapour Deposition (CVD) or Physical Vapour Deposition (PVD) has been the common method contributing to industrial hardened tool steels surface. However, there are several disadvantages of CVD and PVD, namely such high temperature process (distortion problem), sharp edge coating is difficult due to thermal expansion mismatch stresses, limited range of materials can be coated, environmental concerns about process gases and vacuum process with high capital cost (Davis, 2002)

Another widely exercised technique, case hardening boronizing, which is known for its uncomplicated technicality, hardened the surface of steel and enhanced its properties. In boronizing, a boron medium in solid, liquid or gas form supply adequate quantity of atomic boron to be absorbed and diffused into steel at elevated temperature are used.

In conventional gear making, gear part is initially deformed into specific dimension and shape before its hardening process. The complexity of the shape, however, makes it difficult to attain a uniform hardened layer of the gear. Therefore, in this study, shape deformation took place only after the surface hardening process in order to secure homogenity in surface hardness of the component in concern. Furthermore, the process

flow introduced is expected to promote superiority of the gear produced apart from minimizing material wastage.

The ability of a certain material to exhibit large degree of elongations prior to failure known as superplasticity has been recognized for a long time (Choksi, 2005). Superplasticity can also be define as a phenomenon of showing extensive plastic deformation at high temperature in metals. The high ductility achieved through superplastic materials is exploited to form components with complex shapes. It is now being utilized commercially where the scope of applications has extended beyond the aerospace industry that includes the fabrication of many components in the automotive industry (Choksi, 2005).

Meanwhile, Duplex stainless steel (DSS) is widely used in industrial parts such as rotors, fans, shafts and impeler blades due to their their superior corrosion resistance, higher strength relative to other stainless steel (Ahmad et al., 2010). In the last 30 years, DSS has also been studied and characterized as superplastic material (Sagradi et al., 1998).

Previous study on superplastic boronizing of DSS shows that the surface properties of the substrate contributing significant improvement on substrate surface properties (Jauhari et al., 2011). Based on this promising result, this paper is to explore the feasibility of forming boronized DSS into mini gear application through superplastic deformation deliberated under specific spectrums of strains and strain rates. The results gathered therein shall then become the reference in the employment of plastic deformation process after the surface hardening process.

1.2 Objectives

The objectives of this research are:

1) To study the feasibility of forming boronized DSS into mini gear application through superplastic deformation.
2) To evaluate the surface integration of the superplastically boronized duplex stainless steel mini gear formed.
3) To propose optimum strain and strain rate for deformation of boronized duplex stainless steel mini gear.

1.3 Outline of Research

The research outlines are as follows:

1. Understanding the concept and fact
    - The procedure of compression, boronizing process as a surface hardening technique, the concept of superplasticity and the properties of DSS
2. Literature review
    - The theories and concept of superplasticity, boronizing and superplastic boronizing were reviewed from various source such as journals, text books, previous dissertation reports and the World Wide Web. Summary of literatures is presented in Chapter 2.
3. Die design and fabrication
    - A special die for moulding mini gear along with its jigs were designed and fabricated for this study. Material selection of the die for this work was also included in the design. Die drawings was illustrated in Chapter 3.
4. Experimental works

- As received thermo-mechanically treated Duplex Stainless Steel had been pack boronized and subjected to compression process at specified temperature, strain and strain rate to be deformed into mini gear using the special fabricated die and Instron machine as described in Chapter 3.

5. Characterization
    - Hardness of the specimen's boronized surface after boronizing process was measured using Vickers microhardness tester. Thickness measurement and microstructure evaluation were done before and after compression using optical microscope. X-ray diffraction analysis was done to detect the layer formed on the specimen. The characterization techniques were also described in chapter 3.
6. Results and discussion
    - All data obtained from the experiments were compiled and analyzed, and discussed in chapter 4.
7. Conclusions and recommendations
    - Conclusion of this study and recommendation for future research are presented in chapter 5 and 6.

CHAPTER 2

LITERATURE REVIEW

2.1 Superplasticity

Superplasticity was defined as the ability of polycrystalline materials to exhibit in a generally isotropic manner, very high elongations prior to failure (Chandra, 2002) in the international conference on superplasticity (ICSAM-91) in Osaka. A phenomenon by which a material shows very large plastic deformation during tensile loading, under a certain strain rate and temperature can be described as superplastic. Elongations in excess of 200% are usually indicative of superplasticity in tensile deformation of a traditional metal alloys where the normal deformation only up to 20%. Superplastically deformed material gets thinner in a very uniform manner, rather than forming a "neck" (a local narrowing) which leads to fracture (Dieter, 1986)

2.1.1 History of Superplasticity

Although papers on superplasticity occasionally appeared after 1945 (Nieh, et al., 1997), superplasticity work has been found to have begun before 1920. Figure 2.1 shows key discoveries in superplasticity in the early and middle part of the twentieth century prior to major development of interest after 1960.

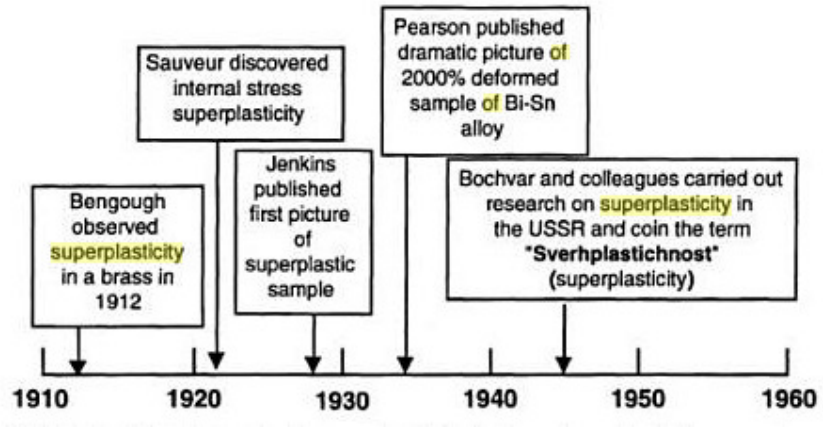

Figure 2.1 Key discoveries in superplasticity before 1960 (Source: Nieh, et al., 1997)

Alloys such as tin/lead and cadmium/zinc displaying abnormally high elongation under low load have been known since the early 1920s (Coiley, 1974). The superplastic phenomena were first highlighted by Rosenhain, Haughton and Bingham on an alloy Zinc-Aluminium-Copper for which they obtained one lengthening of 60%. A tensile elongation of 410% for the Pb-Sn eutectic at room temperature was also reported by Jenkins (Nieh et al., 1997). However, the most spectacular observation was made by Pearson in 1934 which he obtained a lengthening record of 1950% on an alloy Bismuth-extruded tin (Ridley et al., 1992) as shown in Figure 2.2. Pearson had also reported that the size and shape of grains for the superplastic alloys remain unchanged during superplastic deformation. Following these observation, many researches related with superplastic were developed.

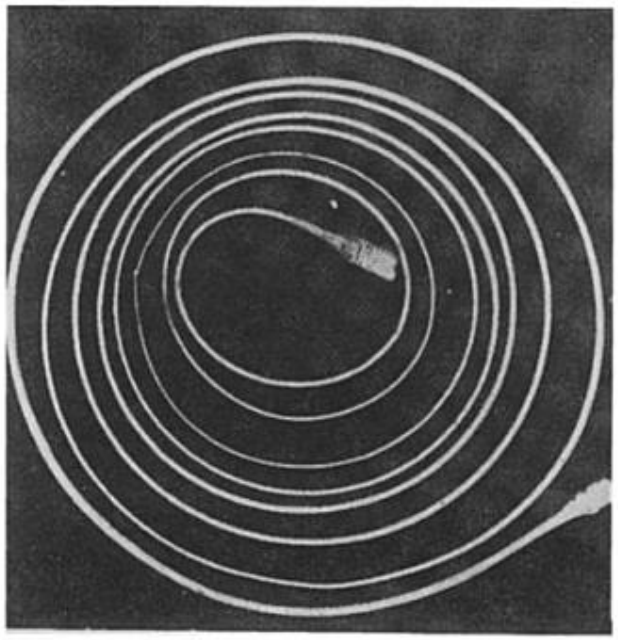

Figure 2.2 Pearson's famous photograph in 1934 of a Bi-Sn alloy that has under gone 1950% elongation. (Source: Nieh, et al., 1997)

Not all materials exhibit superplasticity as had been reported by Chandra (2002). However, a wide range of materials including metals, ceramics, metallic/intermetallic/ceramics matrix composites, intermetallics and nano crystalline materials show superplasticity at some specific loading conditions. Most of these materials do require some special processing condition to achieve the microstructural requirements necessary for superplasticity. Some of these processing were reported by Mabuchi and Higashi (1998). However, some materials such as Ti-6Al-4V alloy already exhibit superplastic behaviour by their commercial process. The current world for elongation in metals stands at 8000% elongation in commercial bronze by Higashi as shown in Figure 2.3.

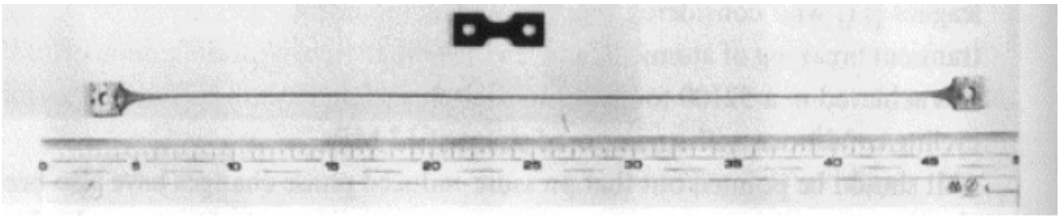

Figure 2.3 A demonstration of superplasticity in Cu-Al alloy with 8000% elongation (source: Chandra, 2002)

2.1.2 Characteristic of Superplasticity

Study of superplastic deformation received much attention because of its attractive behaviour to produce the complex net shape structure at low and intermediate temperature. It was reported by Hertzberg (1996) that superplastic behaviour in most metals, alloys and ceramics are associated with three main characteristic:

(1) A strain rate sensitivity factor m which is more than 0

(2) A fine grain size (on the order1-10μm)

(3) Deformation temperature $>0.5T_m$ (where T_m is the absolute melting point).

2.1.2.1 High Strain Rate Sensitivity

Superplasticity in materials can be evaluated through a number of characteristics and high strain rate sensitivity of the flow stress is the most important characteristic of superplastic deformation. It allows inhibition of necking, which means no localized of failure at a reduced-cross section area. Different materials demonstrate different sensitivity on the strain rate and this is due to the structure of the material. For superplastic alloys, the characteristic mechanical behaviour observed illustrates a strong dependence of flow stress, σ on strain rate, $\dot{\varepsilon}$ at the superplastic temperature. The strain

rate sensitivity exponent referred to as *m* provides a measure of the strain rate sensitivity of flow stress and can be defined by the equation below:

$$m = \frac{\partial (\ln \sigma)}{\partial (\ln \dot{\varepsilon})} \qquad (2.1)$$

Thus, from expressing the flow stress-strain rate relation by the following equation:

$$\sigma = \frac{F}{A} = K\dot{\varepsilon}^{m} \qquad (2.2)$$

Where σ = plastic flow stress m = strain-rate sensitivity factor

F = applied force $\dot{\varepsilon} = \frac{1dl}{1dt} = -\frac{1}{A}\frac{dA}{dt}$ = strain-rate

A = cross-sectional area K = constant

Superplastic behaviour is usually observed when m is usually greater or equal to 0.5 and for most superplastic material m lies in the range of 0.4 to 0.8. Figure 2.4 shows the relation between σ, $\dot{\varepsilon}$ and m.

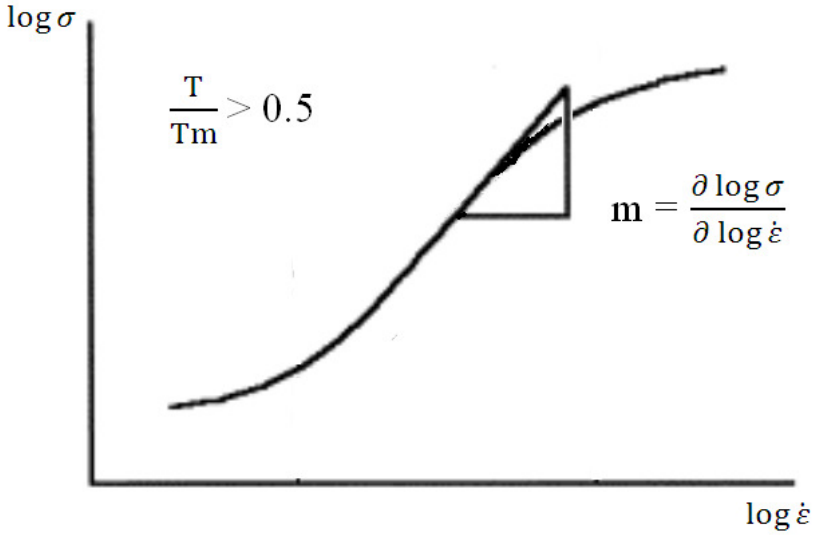

Figure 2.4 Relationship between log stress and log strain with m value

2.1.2.2 Fine Grain Size

Size does matter, and with regard to superplasticity, fine grain size is another main characteristic to be considered. Ductility of materials increases as the grain size becomes finer. In order to create superplasticity in the material or to deform material in the superplastic condition, it is critical for the material to have fine grain structure. Figure 2.5 illustrates that decreasing grain size has an effect on the wider region of the superplastic region. In metals, superplastic behaviour is not normally observed unless the microstructure is fine grained typically 1-10 μm in diameter and the structure must also be stable at the deformation temperature.

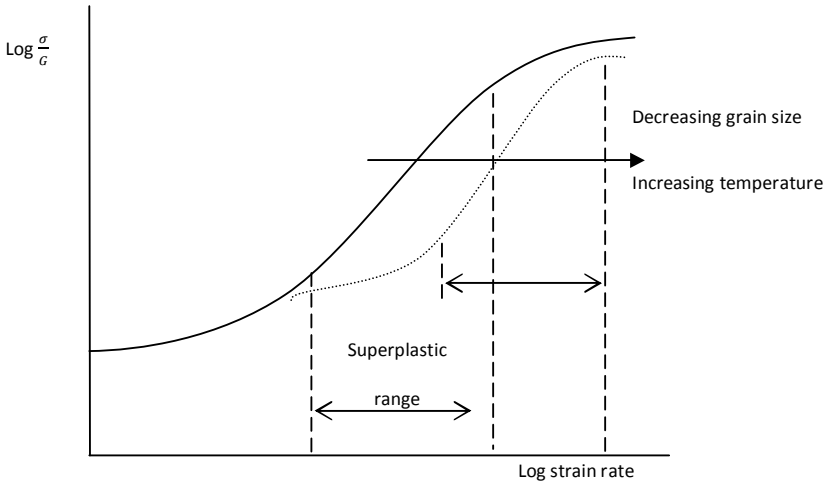

Figure 2.5 Effect of decreasing grain size on the range of superplastic region

2.1.2.3 Temperature

As superplastic behaviour related with the movement of matter, temperature is one of the most important parameter since it is closely related with superplastic deformation and the movement of matter in general. The movement of matter such as the movement of the gas particles, solid particles and water particles is much dependence to

temperature factor. In most materials, superplastic commonly occurs at elevated temperature. The optimal temperature of superplastic forming is systematically higher than 0.5 T_m (T_m is the melting point of material expressed in Kelvin). Most alloys are only superplastic when the deformation temperature is greater than 0.4 T_m. In this condition metal does not experience strain harden due to the equilibrium that co-exists between recovery and hardening.

2.1.3 Mechanism of Superplasticity

Figure 2.6 (a) and (b) shows the evolution of microstructure during superplastic and plastic deformation. In plastic deformation, grains become elongated and the location of neighbouring grain remains unchanged when a tensile force is applied. However, in superplastic deformation grain are observed to change their neighbours and seen to emerge at the free surface from their interior (Chandra, 2002). One characteristic feature of superplastic flow is that grains retain equiaxed or nearly equiaxed shaped after being deformed for several hundred percent elongations (Zelin and Mukherjee, 1996).

(a)

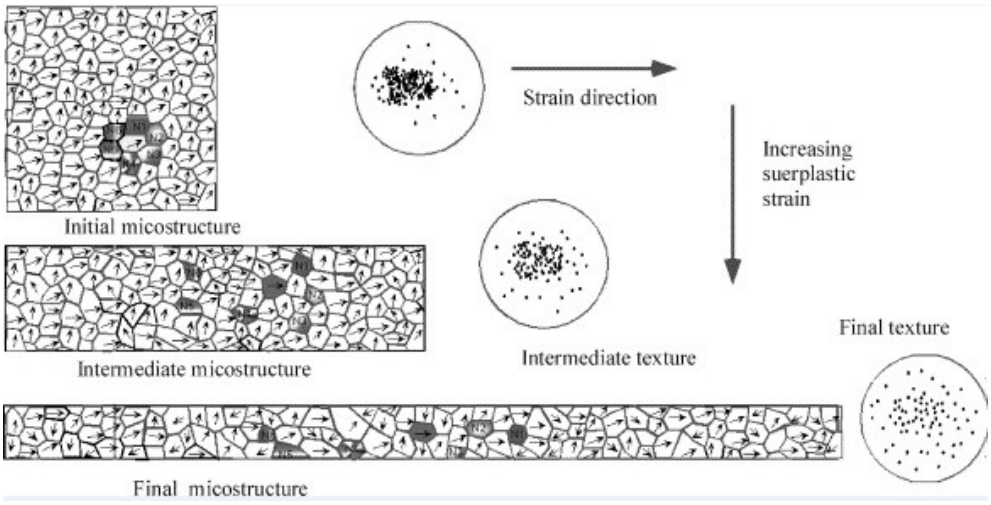

(b)

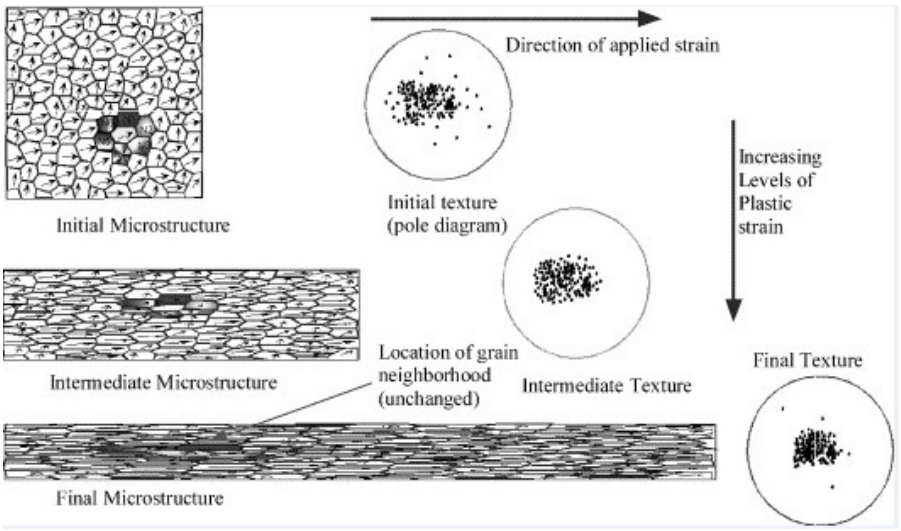

Figure 2.6 Evolution of microstructure during (a) superplastic and (b) plastic deformation (Source: Chandra, 2002)

The exact of superplastic deformation mechanisms have been the subject of interest for a very long time and still not understood properly until nowadays. Several models of mechanism have been proposed for superplastic deformation (Langdon, 1970; Mukherjee, 1971; Gifkins, 1976; Arieli and Mukherjee, 1980; Langdon, 1991; Zelin and Mukherjee, 1996). It is very well established from those studies and researches, that the dominant strain producing mechanism in superplasticity is grain boundary sliding (Chandra, 2002). Strain in a given direction is accumulated by the motion of individual grains and cluster of grain relative to each other by sliding and rolling at the region along the grain boundary surface. Therefore, although there is some difference in grain shape during the accommodation, the grain shape and size remains identical before and after deformation.

The mass flow is due to the diffusion process at the vicinity of grain boundary in diffusional accommodation. When a load is applied to a material, the deformation is due

to grain boundary diffusion and sliding, as a result of strain, as represented by process (a) in Figure 2.7. For accommodation by dislocation motion, it can be understood by dividing the grain into two parts; the core inside the grain, and the mantle at the grain boundary, Figure 2.7 shown (b). In order for the grain to slide, the dislocations which move onto the grain boundary are accumulated at the triple points of the grain boundary. From there, the dislocations move into the mantle due to stress concentration. Thus, the dislocation motion inside the mantle results in the grain rotation. Figure 2.7 (c) shows the process of the accommodation by dislocation motion. The third group of accommodation which combines dislocation and diffusional process is shown in Figure 2.7 (d).

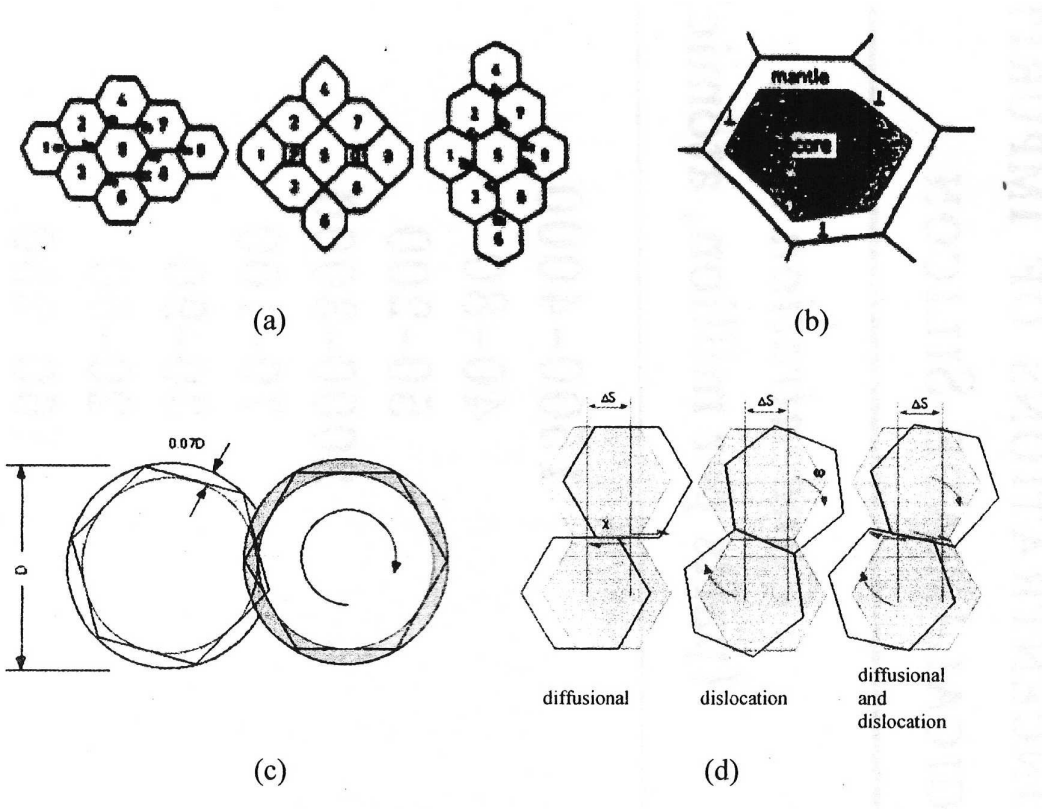

Figure 2.7 Basic accommodation mechanism of superplasticity; (a) diffusional accommodation (b) accommodation by dislocation motion (c) dislocation motion inside the mantle results in the grain rotation (d) combined model with elements of dislocation

and diffusional accommodation (Source (a), (b), (d): Zelin and Mukherjee, 1996; Source 9c); Internet reference-1)

2.1.4 Application of Superplasticity

Superplasticity has been developed and implemented in several application processes (Friedrich and Winkler, 1991; Tsuzuka et al., 1991; Huang and Chuang, 1999; Xun and Tan, 2000; Hefti, 2004; Li and Guo, 2005). Superplastic is mostly being used to form parts in aerospace applications (Xing et al., 1995; Tsuzuka et al., 1991) but nowadays have been further applied in some non-aerospace application as well. There are two major processes in using superplasticity for commercial applications. The first is superplastic forming (SPF) which utilizes large deformability of the superplastic material and the other is superplastic diffusion bonding (SPBD) where good bonding is achieved on the bonding interface as a result of a local superplastic flow.

In aerospace application, superplastic forming is increasingly being used to form very complex geometries. Nickle-base alloy are used to form turbine disc with integral blades while aluminium alloys are fabricated to form low weight and high stiffness air frame control surfaces. Small-scale structural elements are also produced by utilizing the SPF process (Xing et al., 2004). In non-aerospace applications superplastic aluminium alloys has been used in complex surface profiles, decorative panels for internal and external cladding of buildings and also high speed train (Superform Metal Limited, 1998). Aluminium automotive components fashioned using hot blow forming process helps to reduce the weight while it increases the fuel efficiency of today's cars.

Figure 2.8 (a) shows the SPF process and figure 2.8 (b) shows the final product from SPF. Superplastic forming is usually conducted at high temperature and under controlled strain rate. This process is typically obtained with a single-sided die where the sheet is heated at high temperature and the gas pressure applied in order to push the sheet into the tool (Friedman and Luckey, 2004). The simplicity of the dies and the fact that only a single configuration die is suitable often permit a short lead time to produce parts once the design is completed.

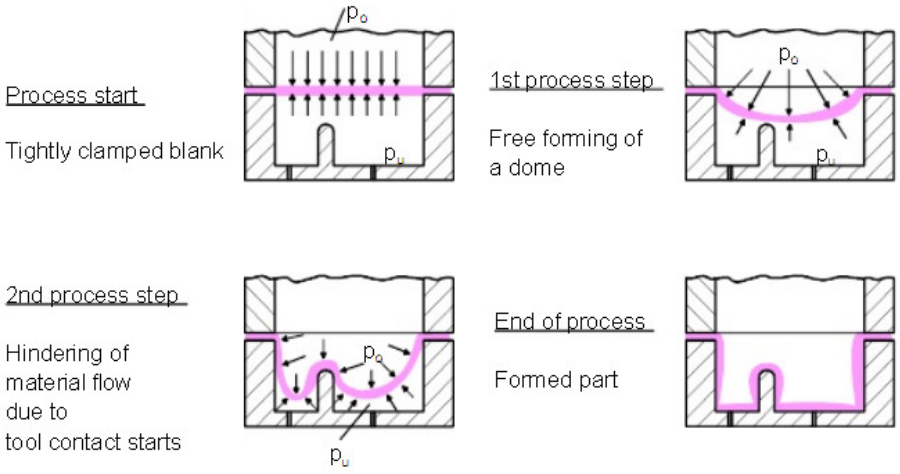

(a)

(b)

Figure 2.8 (a) Superplastic forming (SPF) process (b) SPF formed component (Source: Siegert and Werle, 1994a)

It was reported that superplastic deformation accelerates the solid state diffusion bonding process while obtaining effective bonding (high strength) with minimum material deformation (Jauhari et al., 2002). The acceleration of solid state joining by superplastic deformation is closely related with the development of grain boundary sliding in the material (Lutfulin et al., 1995). SPF together with DB has been implemented to produce hollow engines blades, fan and compressor blades for aero engines (Xun and Tan, 2000; Xing et al., 2004). Figure 2.9 (a) shows the process steps of superplastic diffusion bonding and superplastic forming in the manufacture of a box profile. Figure 2.9 (b) shows a hollow box profile with closed chambers. All these applications reveal the great contribution of well-known superplastic forming (SPF) and superplastic diffusion bonding (SDB) application.

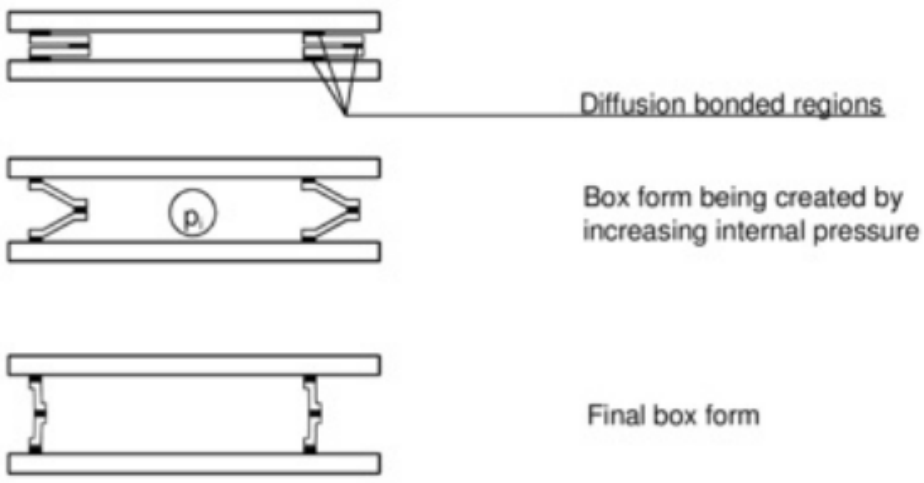

(a)

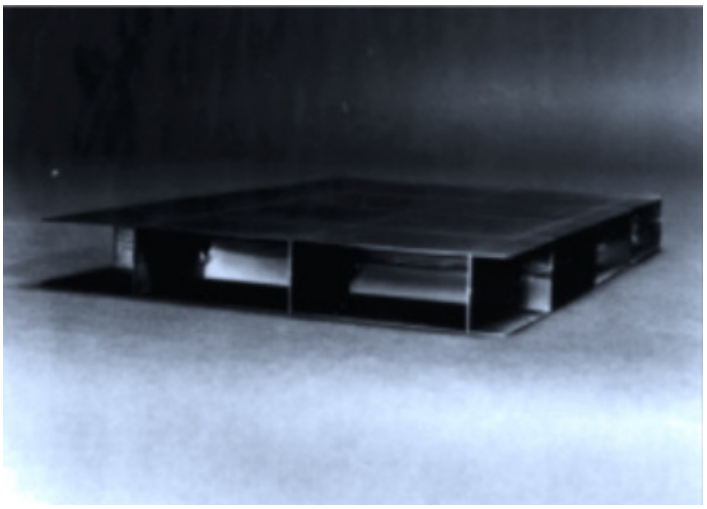

(b)

Figure 2.9 Superplastic diffusion bonding and superplastic forming (SDB/SPF): (a) SDB/SPF process steps (b) SDB/SPF formed component (Source: Siegert and Werle, 1994)

2.2 Boronizing

Boronizing is a thermo-chemical diffusion treatment where the boron atoms are diffused into a metal surface to form metal boride layer that intensifies the sturdiness and durability against wear and tear. Boronizing is well known in enhancing wear resistance of ferrous and non-ferrous alloys. The most relevant element of the thermo mechanical process is the production of a very hard layer that can reach a hardness of exceeding 2000HV, promising a better strength to friction wear and abrasion compared to carburizing and nitriding (Sinha, 1991; Ventaraman & Sundararajan, 1995; Melendez et al., 1997; Meric et al., 2000). Boronizing typically requires process temperatures of 973 K to 1273 K in either gas, solid or liquid media (Genel et al., 2003: Yapar et al., 2004). Keddam and Chentouf (2005) suggested that the powder-pack boronizing has the advantages of simplicity and cost-effectiveness in comparison with other boronizing process. In this technique, the boronizing agent in powder form is placed into a heat

resistant box and samples are embedded into this powder under inert gas atmosphere. It was reported by Jain and Sundararajan (2002) the thickness of boride layer formed is determined by the temperature and time of the treatment. In boronized mild steel, sliding wear can be reduced by up to three orders of magnitude (Biddulph, 1977).

In boronizing process of ferrous alloys, iron borides FeB and Fe_2B are used to be formed. Depending on the boron potential of the pack, single layer of Fe_2B or double phase layer with FeB and Fe_2B may be formed. A single layer is generally better for wear resistance than a duplex layer (Biddulph, 1977). It was reported by Jain and Sundararajan (2002), the boron rich FeB phase (containing approximately 16.23% wt. % B) is not desirable because FeB is more brittle than the iron sub boride, Fe_2B phase (containing approximately 8.83% wt. % B). Furthermore, since FeB and Fe_2B phases exhibit substantially different coefficients of thermal expansion, CTE (α_{FeB} =23 x 10^{-6} / ^{o}C, α_{Fe2B} =7.85 x 10^{-6}), crack formation is often observed at the FeB/Fe_2B interface of a double phase layer which may lead to flaking and spalling when a mechanical load is applied. It is important during pack boronizing process to control the boronizing parameter to ensure Fe_2B phase can be consistently achieved.

Many studies have been carried out on the boronizing treatment in recent years. Most of these studies were based on the use of different materials applied to this process and as a result explain the varying characterization of the obtained surface coating. Allaoui et al. (2006) did studies on XC38 steel, Sahin and Meric (2002) on different cast irons, Ozbek et al. (2000) on nickel. Some other studies examined the effects of treatment parameters on the boronized surface, as well as the mechanical and the technological properties of these boronized materials. Besides, tribological properties of different boronized materials has been investigated by Taktak (2006), Béjar and Moreno (2006), Selçuk et

al. (2003). A significant amount of work has been done on the acquisition of boriding layers, boronizing mechanism, and phase composition of boride layers. Bartsch and Leonhardt (1999), Filep and Farkas (2005) used plasma boriding in order to obtain boride layer. Novakova et al. (2004) achieved a boride layer on low-carbon steel by using electron beam boriding method.

Parallel with earlier mentioned development, few other researchers have worked on the surface roughness of boriding material. It was reported by Jain and Sundararajan (2002) that the initial roughness of the steel sample prior to boronizing ranged from 0.2 to 0.3 μm in Ra, and increased approximately by a factor of 2-3 with boronizing. However, the aforementioned increase in roughness was clearly independent of pack thickness employed. The increase in roughness of the reasonably smooth surface was due to chemical reaction at surface resulting in the formation of iron borides. It was reported that the surface roughness of the sample increased during the boronizing process (Yu et al., 2005).

Table 2.1 shows the typical surface hardness values of boride steels compared with other hard materials. The hardness of boride layers produced on carbon steel is much greater than that produced by any other conventional surface hardening treatments. It exceed that of hardened tool steel, hard chrome electroplate, and is equivalent to that of tungsten carbide. The combination of high surface hardness and low surface coefficient of friction makes a significant contribution in combating the main wear modes; adhesion, tribo oxidation, abrasion, and surface fatigue.

Table 2.1 Typical surface hardness values of borided steels compared with other hard materials (Source: Internet Reference-2)

Material	**Microhardness (HV)**	**Material**	**Microhardness (HV)**
Borided mild Steel	1600	Nitrided Steels	650-1700
Borided H13 Tool Steel	1800	Carburized Low Alloy	650-950
Hardened/Tempered H13	540-600	Hard Chrome Plating	1000-1200
Borided A2 Tool Steel	1900	Cemented Carbide WcCo	1160-1820 (30Kg)
Hardened/Tempered A2	630-700	TiN	2000
Quenched Steel	900	SiC	4000
High-speed Steel BM42	900-910	BC	5000
Diamond	>10,000	-	-

2.2.1 Conventional Boronizing

Boronizing process medium can be either in solid, liquid or gaseous form. Gas offers a number of distinct technical advantages as a diffusion medium, and is used successfully, for example, for nitriding, case hardening and chromizing. However, due to unsolved problems and serious deficiencies that remain un-rectified, gas-phase and liquid-phase

boronizing have not become state-of-art (Internet Reference-3). Therefore, boronizing process technological variants solely based on solid or powder pack boronizing.

Solid boronizing or Powder pack boronizing process is simple, economical, original and industrially reliable (Goeuriot et al., 1981). In the process, the work piece is placed in a suitable container and embedded in the boronizing agent, which is the activated boron carbide. In order to minimize consumption of the latter, the container and the work piece should be of the same shape. To avoid complication, boronizing should be performed in a protective gas atmosphere, which may be pure argon, pure nitrogen or mixture of hydrogen and either argon or nitrogen. This is accomplished either by packing the containers into a protective gas retort and heat-treating them in a chamber furnace, or else boronizing directly in a retort furnace with the necessary protective gas supply (Internet Reference-3). Figure 2.10 shows the schematic of powder pack boronizing.

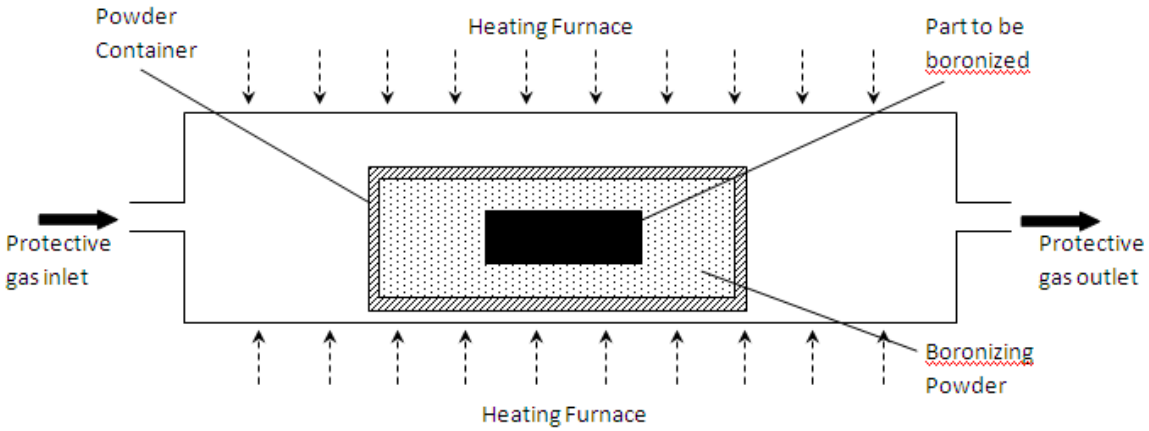

Figure 2.10 Schematic diagram of powder pack boronizing

In powder pack boronizing, the high cost of boronizing agent and protective environment has severely limited its applications. One way to bring down the cost of the boronizing process is to reduce the thickness of the boronizing powder to be packed around the component (called pack thickness) to the minimum required level without

compromising on the properties of the boride coating. A minimum pack thickness of 10 mm is required to obtain boride coatings of optimum thickness, microstructure and properties in low carbon steel (Jain and Sundararajan, 2002)

Meric et al. (2000) had reported that boride layer thickness increased with the decreased in carbon content of the material. Furthermore, it was also found that the boride layer adhere well to carbon steels and high chromium steels but unsatisfactory results were obtained with very highly alloyed steels such as 18010 steel (Goeuriot et al., 1981). In high concentration, alloying elements such as carbon (0%-2%), nickel (0%-14%) and chromium (0%-26%) tend to favour the formation of relatively flat and thin boride layers, even when these layers are highly textured, in contrast with the single-phase acicular Fe_2B layer obtained on low carbon steels, which can penetrate deep inside material. The concentration profiles developed during boronizing revealed different behaviours: carbon segregates towards the matrix, nickel segregates towards the surface, whereas chromium is scarcely affected. The segregation of nickel to the surface at high boron activities severely hinders the successful boronizing of highly alloyed steels, e.g. austenitic stainless steels. (Goeuriot et al., 1982)

2.3 Boronized Materials

2.3.1 Duplex Stainless Steel

Duplex stainless steel (DSS) is defined as a family of stainless steel consisting of a two phase aggregated microstructure of α-ferrite and γ-austenite (Han and Hong, 1999). The balanced 50% α-ferrite and 50% γ-austenite microstructure is obtained by controlled chemical analysis and heat treatment, to produce optimum properties (Charles and

Vincent, 1997). Due to the two-phase microstructure, DSS combine the desirable properties of the austenitic and ferritic stainless steels in such a way that superior resistance to stress corrosion cracking, pitting, crevice and general corrosion (Cabrera et al., 2003). Moreover, it is also has high tensile and fatigue strength, good toughness even at low temperatures, and adequate formability and weldability. These factors promote DSS as suitable alternative to conventional austenitic stainless steel. DSS has become established materials in many industrial applications such as in oil extraction, paper manufacturing and chemical industries (Cabrera et al., 2003; Charles and Vincent, 1997; Tuomi et al., 2000).

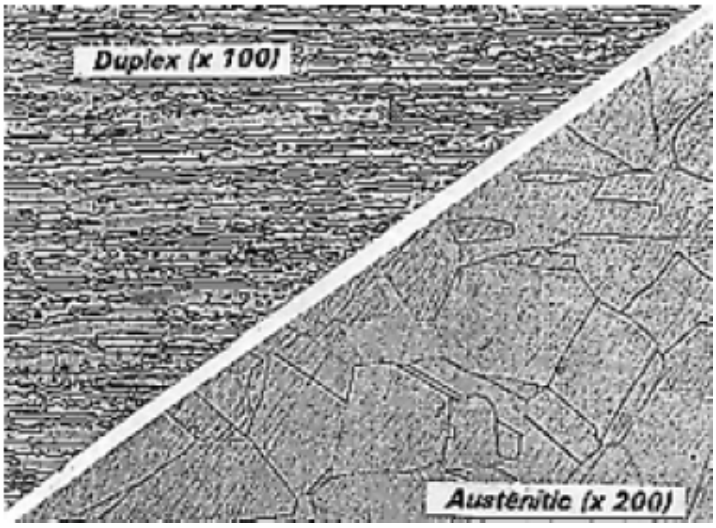

Figure 2.11 Micrographs of both duplex and austenitic stainless steel (Source: Charles and Vincent, 1997)

Figure 2.11 shows micrographs of duplex stainless steel and austenitic stainless steel as for comparison. The duplex microstructure shows a balanced 50% α-ferrite (dark areas) and 50% γ-austenite (light areas). Figure 2.12 shows a phase diagram of Fe-Cr-Ni alloy. As shown in the diagram, duplex stainless steel solidifies initially as ferrite, then transforms on further cooling to a matrix of ferrite and austenite. In order to avoid

formation of brittle intermetallic phases, the usable temperature range of duplex stainless steel is restricted in the range of 223 K to 553 K (Internet Refernce-4).

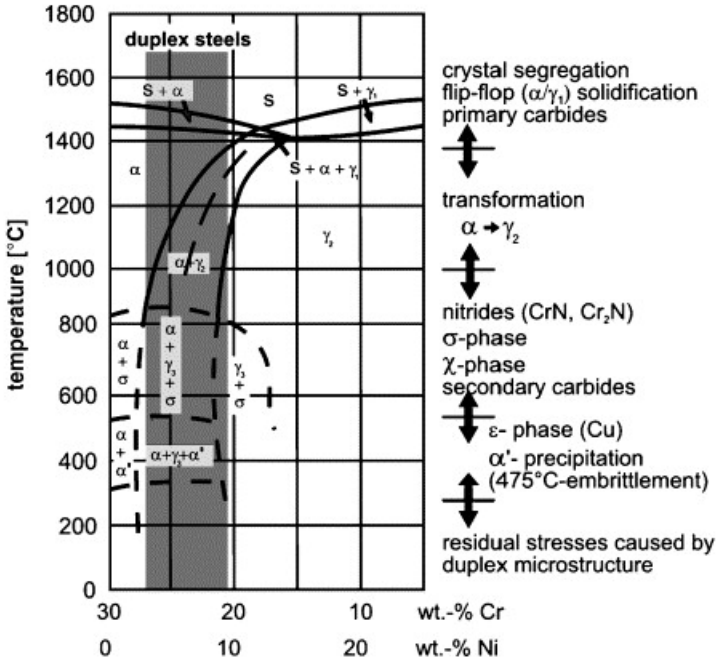

Figure 2.12 Fe-Cr-Ni phase diagram (Source: Michael et al., 2007).

2.3.2 Superplastic Duplex Stainless Steel

Duplex stainless steel (DSS) have been studied and characterized as superplastic materials in the last 30 years. It was reported by Han and Hoong (1999) that duplex stainless steel with fine grain microstructure has ability to show superplastic behaviour since the grain growth is effectively suppressed at high temperature due to the two phase aggregated microstructure. It is known that the processing steps providing the finest microstructures which are stable at the deformation temperature and would enhance superplasticity are definitely important since a fine-grained microstructure is the most important feature of superplastic materials.

In duplex stainless steel processing, there are several practices of thermo-mechanical techniques to develop a superplastic microstructure. Thermo-mechanical process consist of hot rolling the material in temperature range of 1100-1300^{o}C followed by cold rolling with 50% reduction (Jimenez et al., 2001) is one of the example. The tensile elongation of superplasticity deformed duplex stainless steel increased with increasing amount of reduction during cold rolling (Han and Hong, 1997). The fine grained duplex microstructure is obtained through the precipitation of the second phase particles when the thermo-mechanically treated duplex stainless steel is heat up at test temperature (Han and Hong, 1999). Figure 2.13 shows microstructure of thermo-mechanically treated duplex stainless steel with grain sizes of about 10μm after it has been heated up at test temperature ranging from 858 to 1000^{o}C.

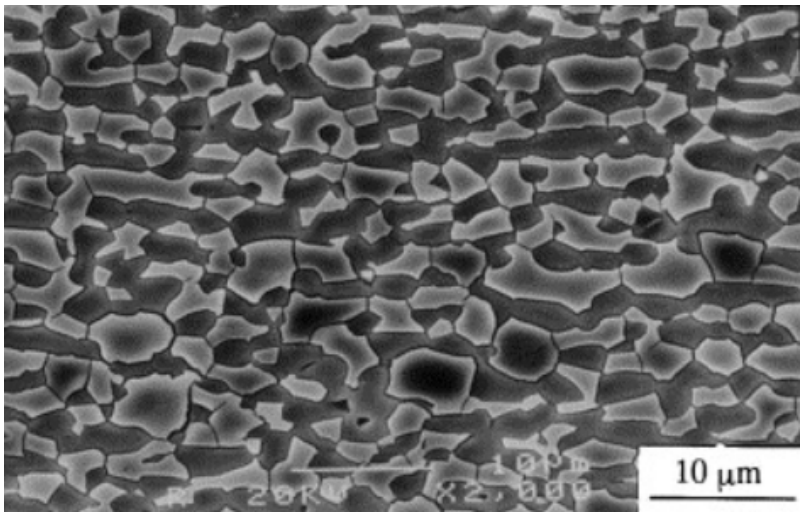

Figure 2.13 Microstructure of fine grain duplex stainless steel (Source: Miyamoto et al., 2001)

The micro structural evolution during deformation identifies grain boundary sliding as the mechanism responsible for superplastic deformation of duplex stainless steels (Jimenez et al., 2001). On the other hand, some previous studies suggest that the

dynamic recrystallization of the softer phase in duplex stainless steel or other duplex microstructure, which occurs continuously during deformation, could be the dominant mechanism for superplasticity at temperature range 800-1100^{o}C. However, Tsuzaki et al. (1996) suggested that grain boundary sliding is the dominant mechanism for superplasticity in duplex stainless steel and that the role of dynamic recrystallization is to keep the grain size fine, suitable for grain boundary sliding. Furthermore, it also concluded that the grain boundary assisted by dynamic recrystallization is considered to be the controlling mechanism for superplastic deformation of DSS (Han and Hong, 1999)

2.4 Boronizing Agent

The only boronizing agents of industrial importance are those based on activated boron carbide. They can be purchased as fine powders, as grain of various sizes, and as pastes. The Ekabor TM boronizing agents supplied by BorTec are listed in Table 2.2. The main constituents are the boron donor, the activator and the filler.

Table 2.2 EKABOR^{TM} boronizing agents (Source: Internet Reference-3)

Boronizing Agent	**Grain Size (μm)**	**Comment**
EKABOR^{TM} 1	<150	Highest-quality surface layer; tends to bond
EKABOR^{TM} 2	<850	Very good surface layer; the part is easy to unpack after treatment
EKABOR^{TM} 3	<1400	Good surface layer; powder still has good flow properties after treatment
EKABOR^{TM} HM	<150	For hard metals, small bore sizes and thick boride

		layers; very good surface layers
EKABOR™ Paste	-	Universal application: immersion, brushing and spraying
EKABOR™ Ni	<150	For boronizing nickel-based materials

Meric et al. (2000) concluded that particle size of the powders used in boronizing was a significant processing parameter and in their study the size of powder decreased with the increased boride layer thickness.

CHAPTER 3

EXPERIMENTAL PROCEDURE

3.1 Substrate Material

Duplex Stainless Steel (DSS) with proportion of 50% α-ferrite and 50% γ-austenite was used as the material for this research. Table 3.1 shows the chemical composition of the DSS (JIS SUS329J1) used in this study. The DSS are prior thermo-mechanically treated through heating up the DSS until 1573K, holding for one hour and followed by water quenching. It is then cold rolled to a plate through a reduction area of 75% shown in Figure 3.1.

Table 3.1 Chemical composition of duplex stainless steel (JIS SUS329J1) in wt %

Element	C	Si	Mn	P	S	Ni	Cr	Mo	Fe
Wt %	0.06	0.42	0.30	0.03	0.06	4.18	24.5	0.49	Bal

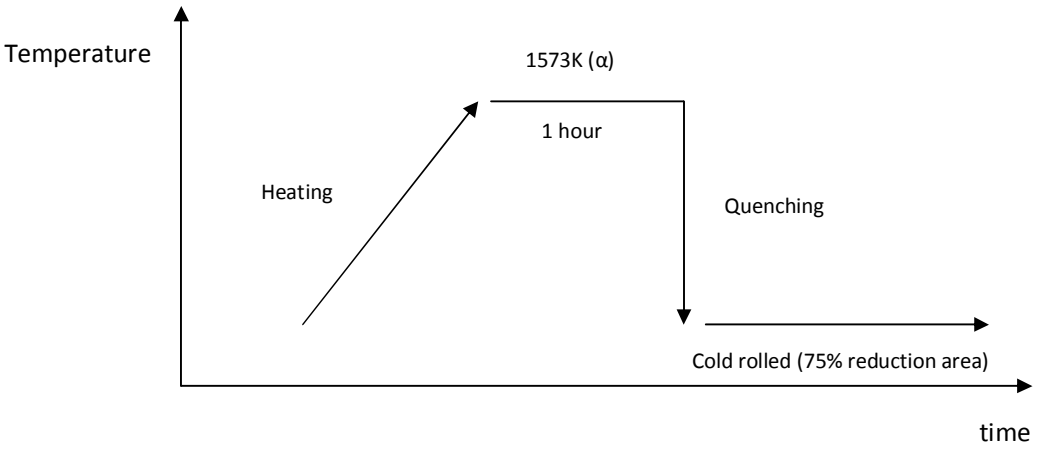

Figure 3.1 Thermo mechanically treated DSS preparation

It was reported that the thermo-mechanically treated DSS showed a superplastic elongation of 1050% at temperature of 1223 K and tensile strain rate of 1 x 10^{-2} s^{-1} as shown in Figure 3.2 (Ogiyama et al., 2001)

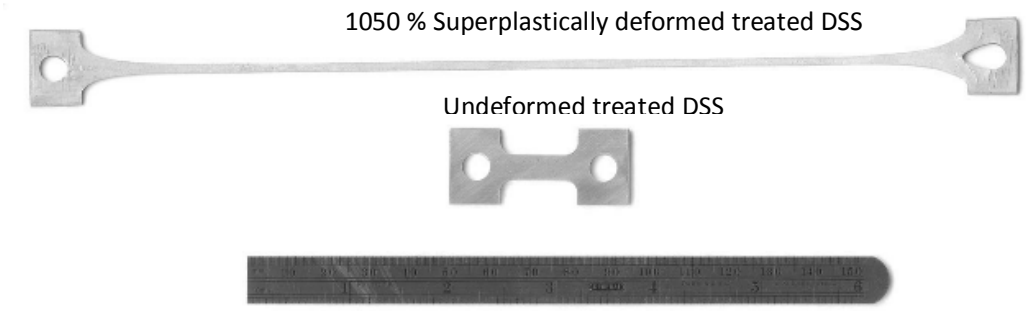

Figure 3.2 The undeform (bottom) and 1050% superplastically deformed (top) thermo mechanically treated DSS (Source: Ogiyama et al., 2001)

3.2 Material Preparation

The thermo mechanically treated DSS plate was cut into cylinder shape specimen with diameter dimension of 12.3 mm and thickness of 3.3 mm using wire-cut machine so that the cutting surface have a relatively high degree of smoothness and flatness as compared to many other cutting method. Figure 3.3 shows (a) the specimen after the wire-cut process and (b) dimension of specimen.

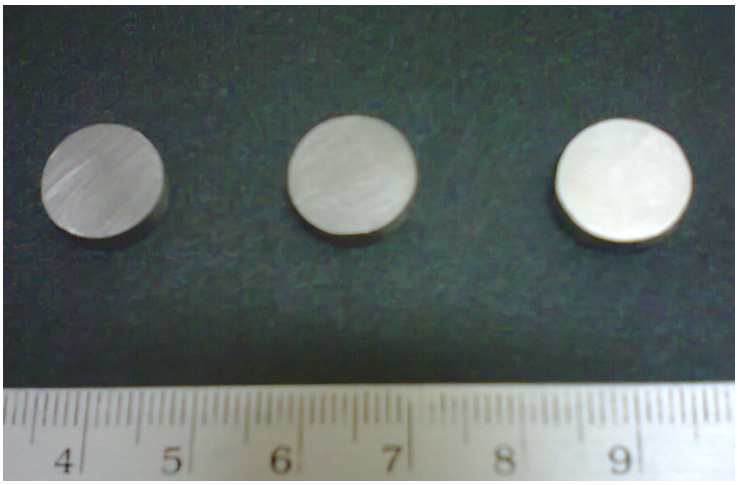

(a)

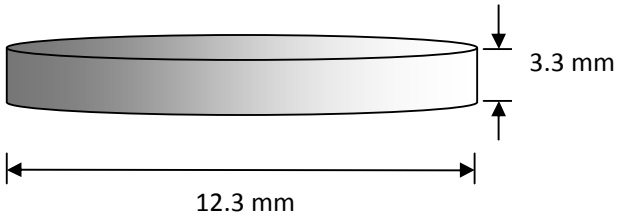

(b)

Figure 3.3 (a) DSS specimen after wire cut process and (b) dimension of specimen

After the cutting process, the whole specimen surface was ground by using 240-grit emery paper. The grinding works was performed by using Struers RotoPol-31 grinding and polishing machine shown in Figure 3.4

Figure 3.4 Struers RotoPol-31 Grinding and polishing machine

3.3 Design and Fabrication of Die Set

In order to conduct superplastic deformation of the boronized substrate so to sculpt the designed gear form, a specially designed die set was fabricated as shown in Figure 3.5 (a) and (b).

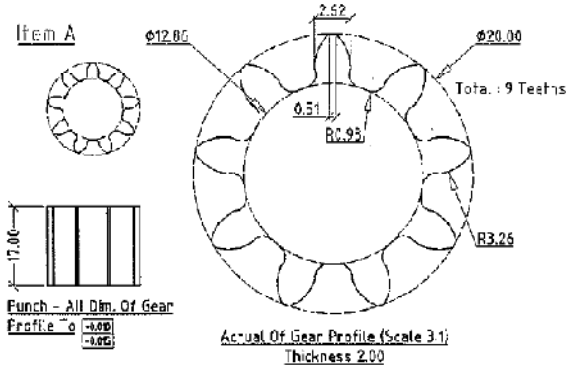

(a)

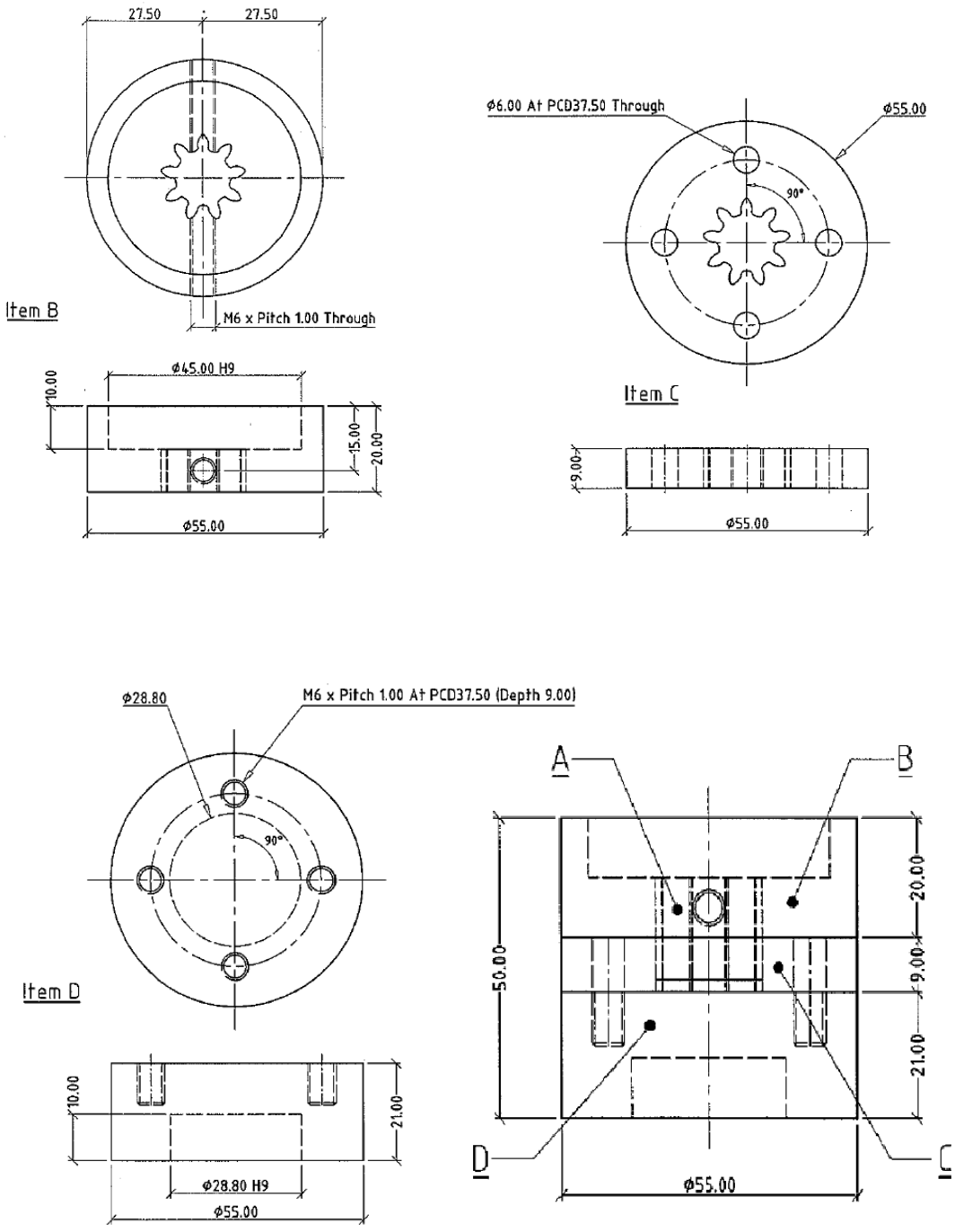
27.50
27.50
Item B
M6 x Pitch 1.00 Through
ø45.00 H9
10.00
15.00
20.00
ø55.00
ø6.00 At PCD37.50 Through
ø55.00
90°
Item C
9.00
ø55.00
ø28.80
M6 x Pitch 1.00 At PCD37.50 (Depth 9.00)
90°
Item D
10.00
21.00
ø28.80 H9
ø55.00
A
B
D
C
50.00
20.00
9.00
21.00
ø55.00

(a)

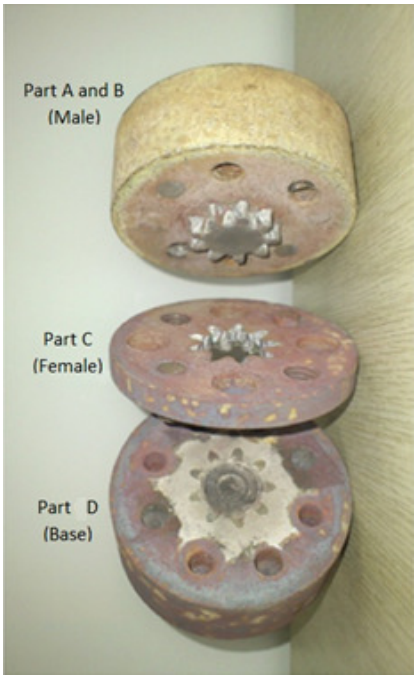

(b)

Figure 3.5 (a) Mini gear Die set drawing (b) Actual Die set Fabricated

Properties of materials that determine their selection as die materials for hot forging are: ability to harden uniformly, wear resistance (ability to resist the abrasive action of hot metal during forging), resistance to plastic deformation (ability to withstand pressure and resist deformation under load), toughness, resistance to thermal fatigue and heat checking, and resistance to mechanical fatigue (Semiatin et al., 1998). The material used in fabrication of die set was Chromium-base AISI hot work tool steels H 13.

3.4 Design and Fabrication of Jig Set

A specially designed jig set was also fabricated for the mini gear formation process. Figure 3.6 shows the schematic of the jig set designed for this work. Stainless steel was selected for this jig set with respect to its high resistance to corrosion (rusting) in miscellaneous atmospheres especially in ambient temperature. Besides, stainless steel is also frequently used at elevated temperature and in severe environment because they

resist oxidation and maintain their mechanical properties under such conditions (the upper temperature limit in oxidation atmospheres is about 1273 K). Both die set and jig set were then set up in Instron machine for the mini gear deformation process.

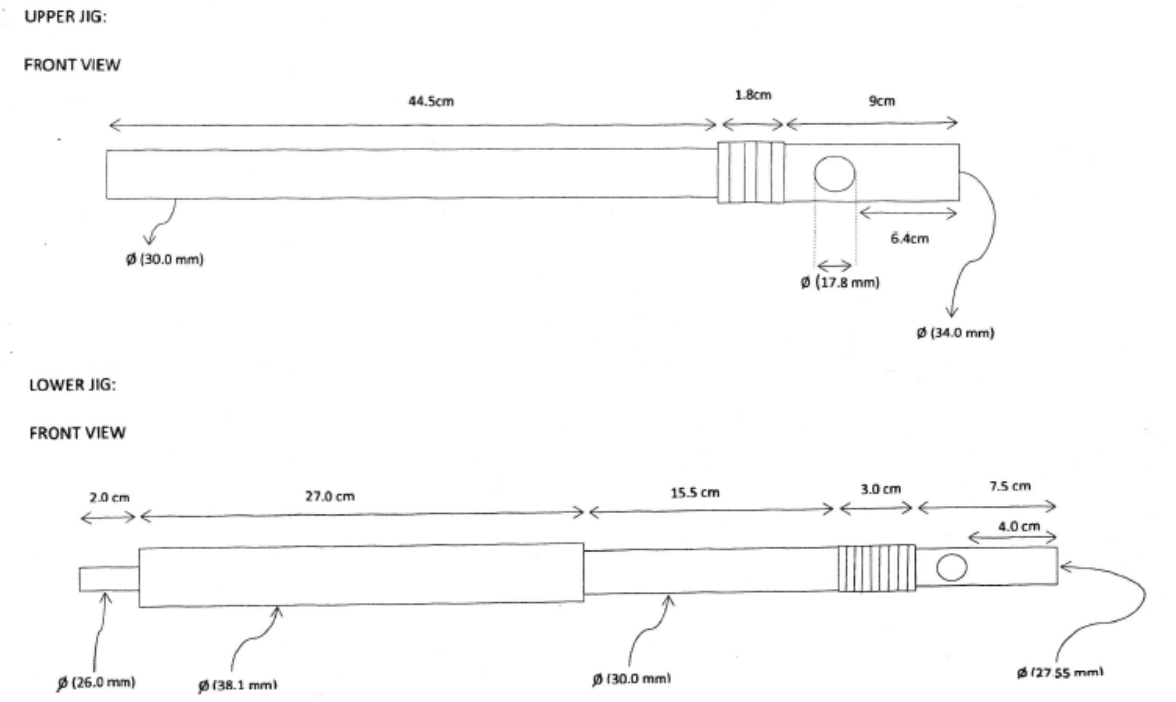

Figure 3.6 Schematic diagram of the jig set designed for this work

3.5 Boronizing Process

After the cutting process, the samples are pack-boronized with boron powder (Ekabor-1) in a stainless steel container schematically shown in Figure 3.7. Commercial Ekabor-1 powder by BoeTec Germany was used as the boronizing agent. The boronizing process was performed at 1223K for 6 hours in a tube furnace as shown in Figure 3.8 with controlled atmospheric condition using argon gas. After the boronizing process has finished, the sample is furnace-cooled to room temperature.

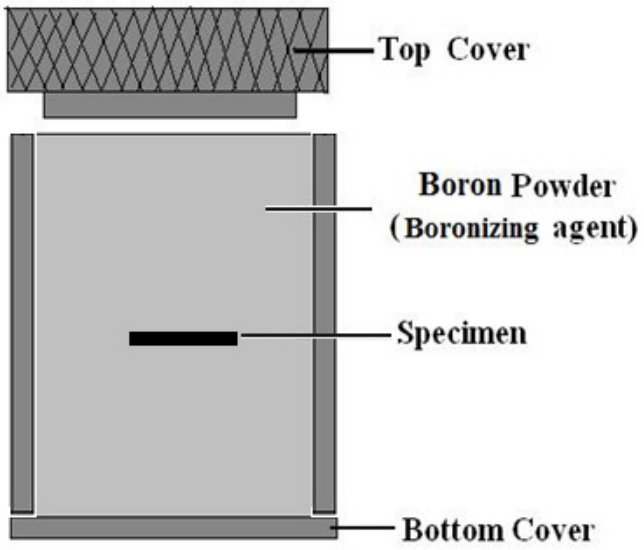

Figure 3.7 Schematic diagram of conventional boronizing

Figure 3.8 Tube furnace with controlled atmospheric condition using argon gas used for the boronizing process

3.6 Superplastic Deformation

Forming was conducted to the boronized samples using a compression testing machine (Instron) equipped with high-temperature furnace under argon gas as shown in Figure 3.9. The sample was put in the die set and the die set was placed above the lower jig. The lower and upper jig was then inserted into the furnace. Figure 3.10 shows the detail of this experimental set up.

Figure 3.9 Instron machine used for the sample compression

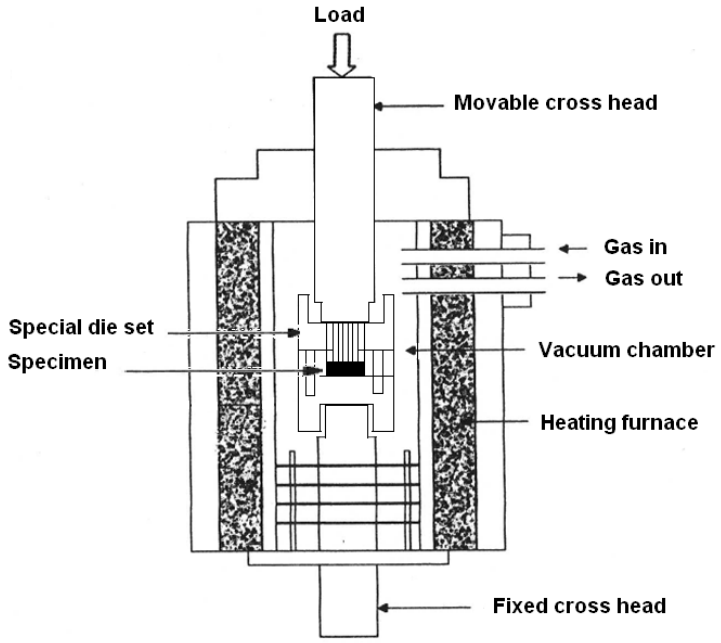

Figure 3.10 Experimental set-ups for the superplastic deformation process

Superplastic deformation for this mini gear formation was carried out at 1223 K. Water is allowed to flow towards the pulling rod to prevent the system from overheating. Once the thermal reading hit the required temperature of 1223 K, the specimen was held for 1 hour to ensure that homogenous heating was achieved and fine microstructure was well formed. After that, upper jig was lowered until it touched the specimen in the die set. The specimen was the prepared for superplastic deformation test with different strain and strain rate as summarized in Table 3.2.

Table 3.2 Summary of experimental conditions for deformation

Sample	Strain (mm/mm)	Strain Rate (s^{-1})	Deformation Time (s)
A	0.4	1×10^{-4}	4000
B	0.4	6×10^{-5}	6666
C	1	6×10^{-5}	16666

After deformation process was completed, the upper jig was held at the final level to avoid any retraction within the formed mini gear specimen as final strain was being applied. The specimen was then allowed to cool in furnace. After the furnace temperature declined to room temperature, the upper jig was raised up and the specimen was taken out for further characterization. Figure 3.9 shows time frame of superplastic deformation testing.

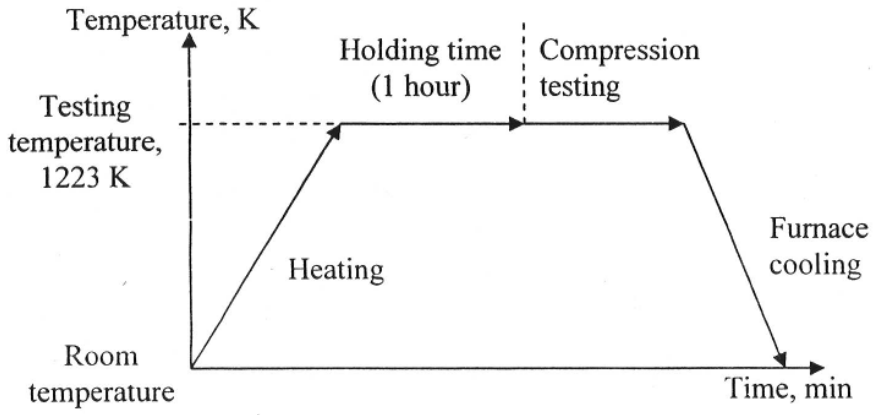

Figure 3.11 Process flow diagram of superplastic deformation testing

3.7 Characterization method

Further investigation on the macro- as well as micro-structure of the specimen entailed a number of characterization assessment. X-ray diffraction analysis (XRD) was conducted to confirm the presence of boride phase on the boronized layer, whereas the microstructure of the work piece was studied using the optical microscope and scanning electron microscope (SEM). The surface hardness was also measured after boronizing process. For microscopic study, the specimens were mounted and ground with several grades of emery papers, starting from the coarsest to the finest. Then, the surface was polished with alumina powder until “mirror like surface” were produced. After that the specimen were etched with the etching solution (HCL saturated with $FeCl_3$ activated

with small amount of HNO_3). Figure 3.12 shows mounted specimens ready for examination purpose.

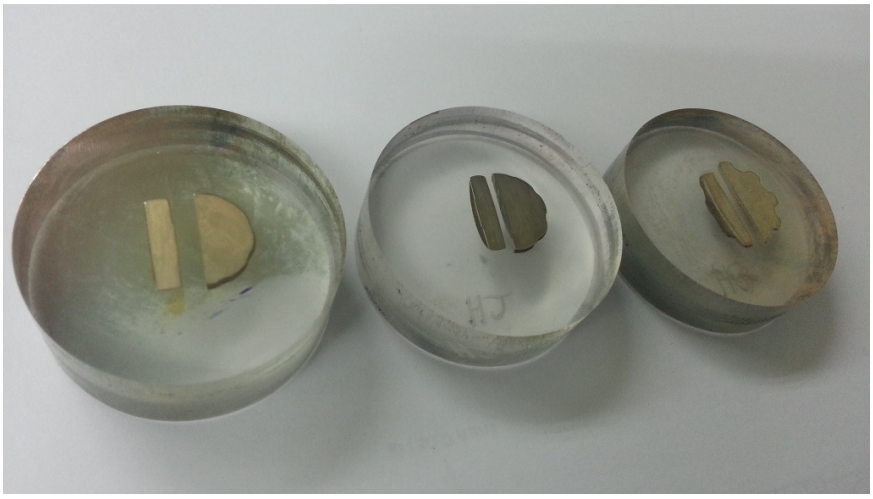

Figure 3.12 Mounted specimens ready for micro examination purpose

3.7.1 X-ray Diffraction

X-ray scattering techniques are a family of non-destructive analytical techniques which reveal information about the crystal structure, chemical composition, and physical properties of materials and thin films. These techniques are based on observing the scattered intensity of an X-ray beam hitting a sample as a function of incident and scattered angle, polarization, and wavelength or energy (Internet source 5).

Philips X'pert MPD PW3040 X-ray diffraction machine with CuKα radiation at 1.54056 Å wave lengths was used in this study as shown in Figure 3.13. The surface of the specimen to be characterized were cleaned with alcohol and placed onto the glass slide. The prepared sample was then put into the sample chamber of the XRD machine for characterization purpose.

Figure 3.13 X-ray diffraction (XRD) analysis machine (Internet Refernce-6).

3.7.2 Optical Microscope

The use of uses visible light and a system of lenses to magnify images of small samples optical allows a wealth of information to be obtained. Material surface treatment was able to be identified and characterized via optical microscopy analysis. It was reported by Zainul (2004), in a reflected light microscope, the specimen was illuminated by frontal lighting, which had been accomplished by means of a small plain-glass reflector placed inside the tube of the microscope.

The optical microscope Zeiss Axiotech with maximum 1000 times enlargement was used in this study. The microscope was equipped with Carl Zeiss AxioCam camera and connected to an image analyzer with AxioVision software as shown in Figure 3.14.

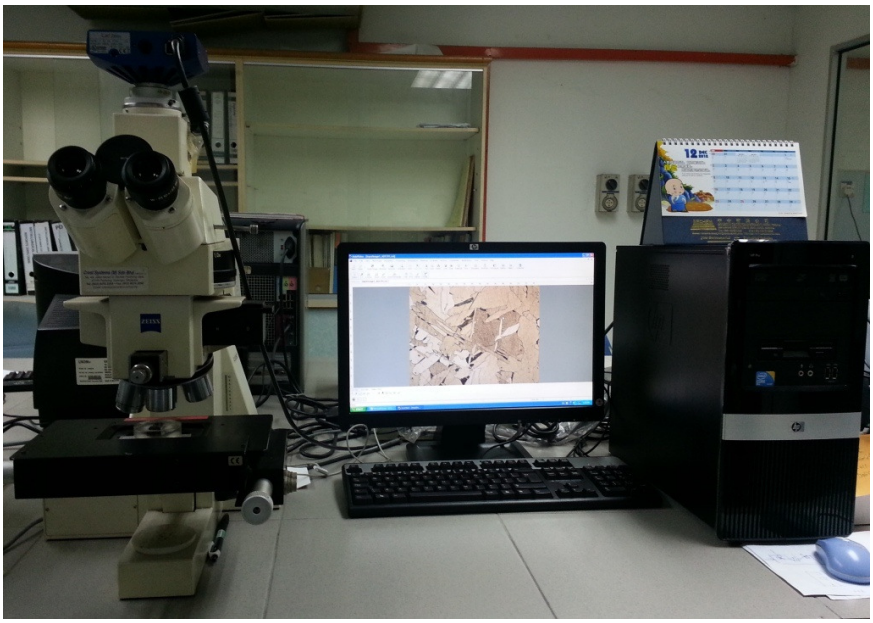

Figure 3.14 Zeiss Axiotech optical microscope with image analyzer

3.7.3 Scanning Electron Microscopy

The difference between optical microscope and scanning electron microscope (SEM) is that the former uses light for imaging purpose. Conversely, SEM uses a beam of electron to capture the image the specimen and gain information as to its structure and composition. The broad scanning dimension of an SEM allows a large amount of samples to be in focus at once. The SEM also able to examine a close space features through its high resolution images. Specimen preparation is necessary before taking SEM image because SEM operates in a vacuum and rely on electric fields to work. Preparation of the specimen is relatively easy since most SEMs only required being conductive. The specimen to be analyzed is mounted on a resin, polished and etched. Then the mounted specimen is connected to the specimen stub using conductive carbon cement which enables the excess electron to flow out from the specimen. The prepared stub is then placed onto the SEM stage in the SEM chamber for analysis. In this study, a Philips model XL40 SEM was used as shown in Figure 3.15.

Figure 3.15 Scanning electron microscope (Internet Refernce-7).

3.7.4 Micro Hardness Tester

The resistance of material to indentation is a qualitative indication of its strength. The microhardness test method according to ASTM E-384 specified a range of loads using a diamond indenter to make an indentation, which is measured and converted to a hardness value. The micro hardness test procedure is almost similar to standard Vickers hardness test except this microhardness test is done on a microscopic scale under higher precision instrument with usage of microscope to measure the indentation.

In this study, after boronizing process, the hardness of treated surface and cross section of boronized specimen from the boronized area to the core of the specimen was measured using Mitutoyo micro hardness tester model MVK H2 with load of 200g (2N) as shown in Figure 3.16. Two diagonals of the indentation were left on the surface of the boronized specimen after removal of the load and thus measured. The figures returned were later implemented for automatic calculation of the hardness reading.

Figure 3.16 Microhardness Tester

CHAPTER 4

RESULTS AND DISCUSSION

4.1 Substrate Material

In this study, as received thermo mechanically treated Duplex Stainless Steel (DSS) with elongated grain microstructure after a 75% cold reduction to its surface area was used. The optical and SEM microstructure image of the specimen before boronizing process shows in Figure 4.1 (a) and (b).

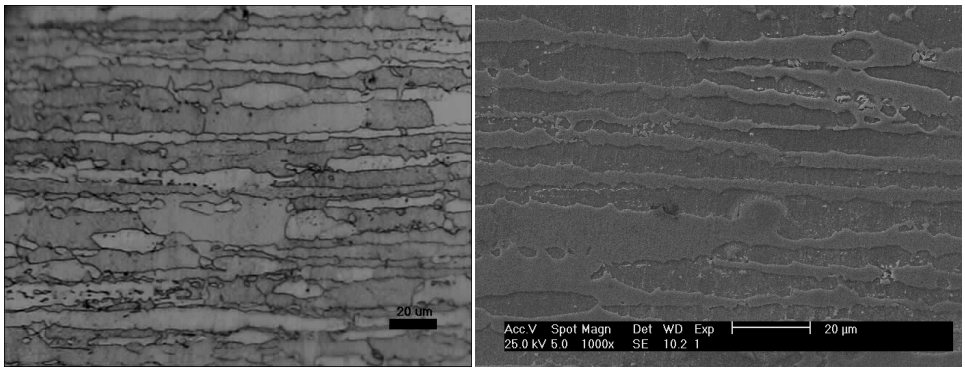

(a) (b)

Figure 4.1 (a) Optical image of as-received DSS (b) SEM image of as-received DSS

Figure 4.2 (a) and (b) shows the optical and SEM microstructure image of the specimen after treated at boronizing temperature.

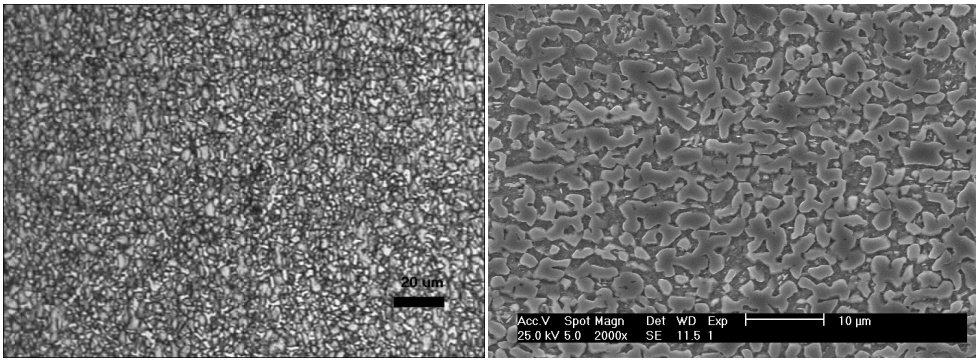

(a) (b)

Figure 4.2 (a) Optical image of fine microstructure DSS (b) SEM image of fine microstructure DSS

After boronizing process, the specimen was then characterized to ensure the presence of boride phases, thickness of the layer and the micro hardness of the layer.

4.1.1 Boride Phases

The presence of boride phases on the boronized specimens were confirmed by X-ray diffractions (XRD) analysis. Figure 4.3 shows the result of XRD on the boronized specimens before and after boronizing process for 6 hours at 1223K. From the figure, the relative peak intensity in the XRD pattern shows the presence of boride phases of FeB and Fe_2B. This result substantiates the success of the process executed on the DSS interface.

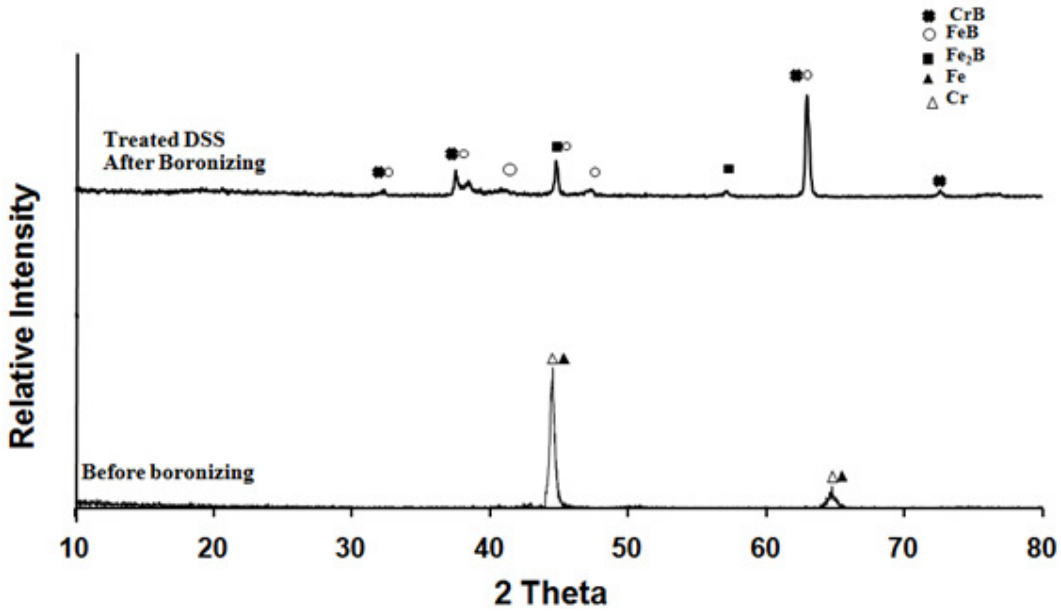

Figure 4.3 XRD pattern of the specimen before and after boronizing process.

4.1.2 Boronized Layer Thickness

Boron layer thickness after boronizing process on the specimen surface was measured using optical microscope as shown in Figure 4.4. The optical image illustrate boronized layer formed on the steel surface having smooth and compact morphology, which can be attributed to high alloying element in DSS. It was reported that alloying elements especially chromium and nickel modify coating-substrate interface by changing the diffusivity of boron atoms (ozbek et al., 2002; Ozbek et al., 2004). Therefore, the morphology of the structure becomes more compact and smoother as the alloying elements were higher. From the result obtained, the boronized thickness layer ranging from 40 µm.

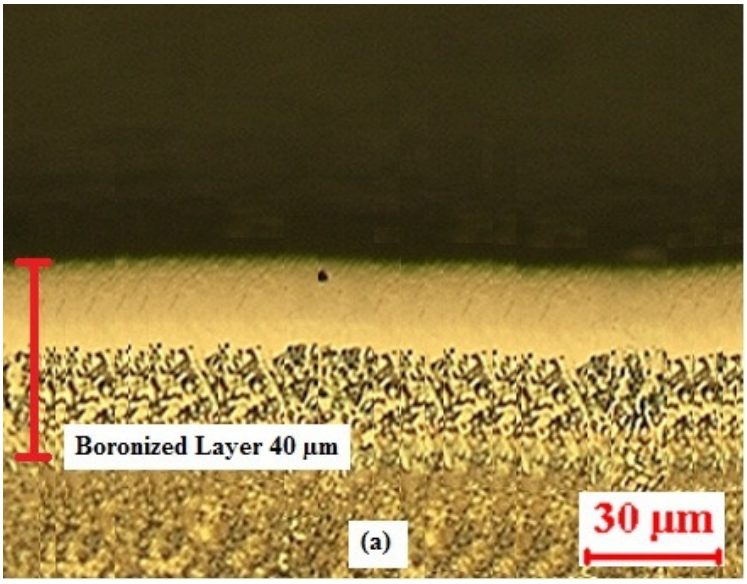

Figure 4.4 Optical images of thermo-mechanically treated after boronizing process.

4.1.3 Boronized Layer Hardness Profile

In this study, the hardness of boronized layer can be determined through its profile from the surface area to the internal as shown in Figure 4.5 and Figure 4.6. From the cross section hardness, it can be observed that the hardness of the boron layer is significantly higher as compared to the substrate material, thus confirming the hardening effect of the process. The highest hardness value was obtained at the boronized layer nearest to the boronized surface area as expected.

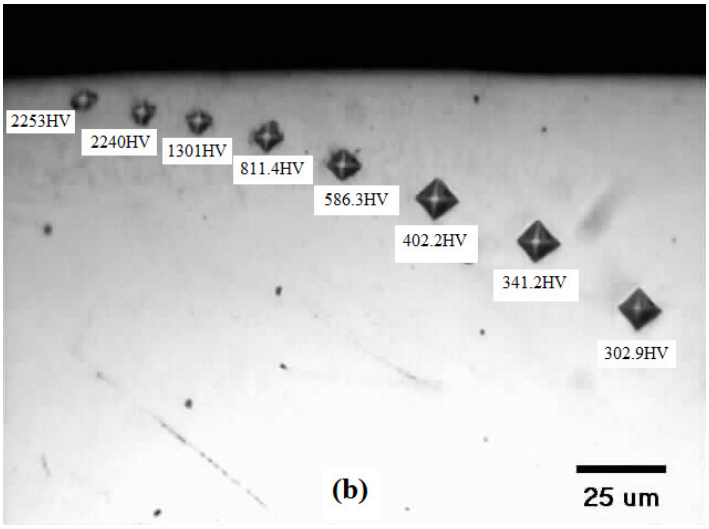

Figure 4.5 Micro hardness profiles on the boronized layer.

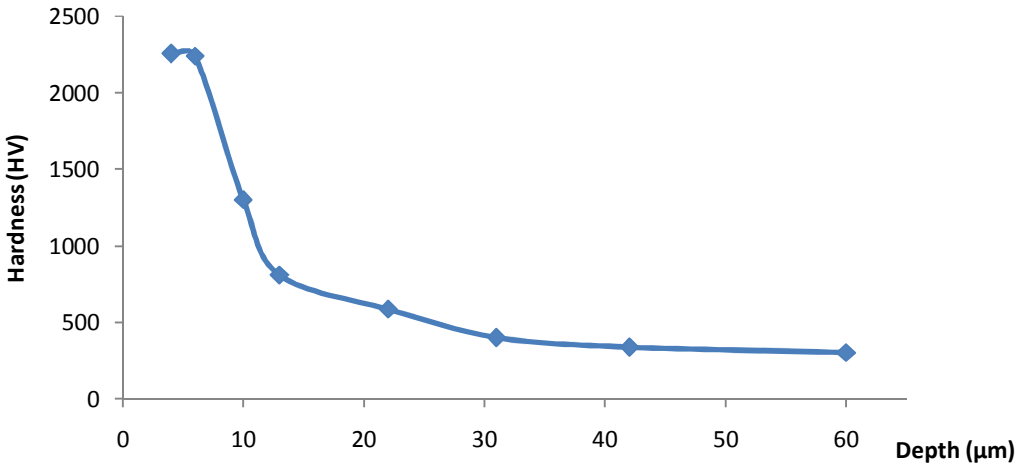

Figure 4.6 Cross section hardness profiles of boronized DSS as a function of depth

4.2 Forming Process

Figure 4.7 shows the plane view of the samples after forming process. It is apparent in this photographic presentation that at a strain rate of 6 x 10^{-5} s^{-1}, the sample C has excellent compressibility and can be perfectly deformed without macro surface disintegration up to strain of 1.0 mm/mm.

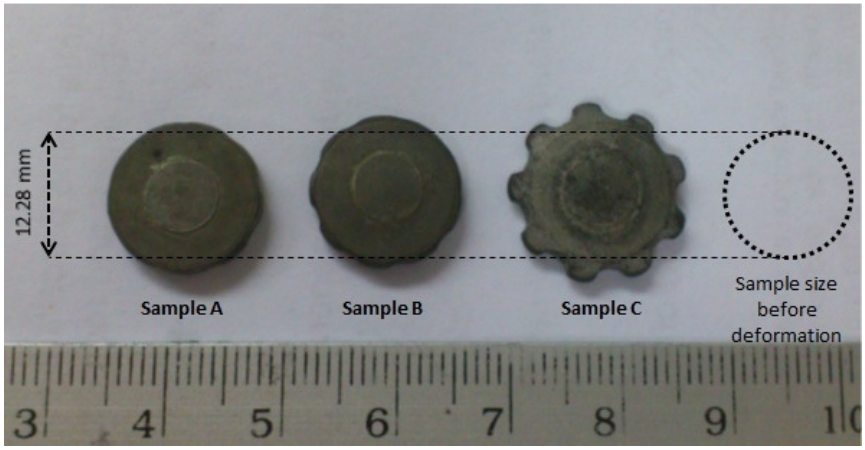

Figure 4.7 Plane view mini gear sample after deformation Sample A: Strain = 0.23 mm/mm, Sample B: Strain = 0.4 mm/mm and Sample C: Strain = 1.0 mm/mm.

4.2.1 Flow Stress Behaviour

Figure 4.8 shows the flow stress of the samples deformation at different strain and strain rate. From the figure, at strain of 0.23 (L_{023}), flow stress of sample B and sample C are lower than sample A. This comparison shows that the flow stress produced increased when the strain rate is increased. It has been understood that superplastic deformation in metals/alloys was closely related to DRX (Prasad, 1998). The degree of DRX increases with the decrease of strain rate. This is because DRX (involving nucleation and grain growth) need time. When strain rate is relatively low, DRX grains have more time to

nucleate and grow. At high strain rate, the accumulated energy increases, as dislocations have not enough time to consume or continually generate. The presence of excess dislocation can lead to heterogeneous nucleation of DRX grains. However, diffusion cannot proceed completely and DRX grain growth is not pronounced because of the very short deformation time. In accordance with the micro structural evolution, the flow stress increases with the increase of strain rate. Thus, it can be concluded that the lower the deformation strain rate, the easier the process of DRX for the alloy while other parameters are consistent. Comparison between Samples B and C demonstrate the effect of different strain. It shows that flow stress is almost similar for both samples even though the strain applied to Sample C is higher. Flow stress plays an important role in maintaining the surface integrity that will be discussed in the later section.

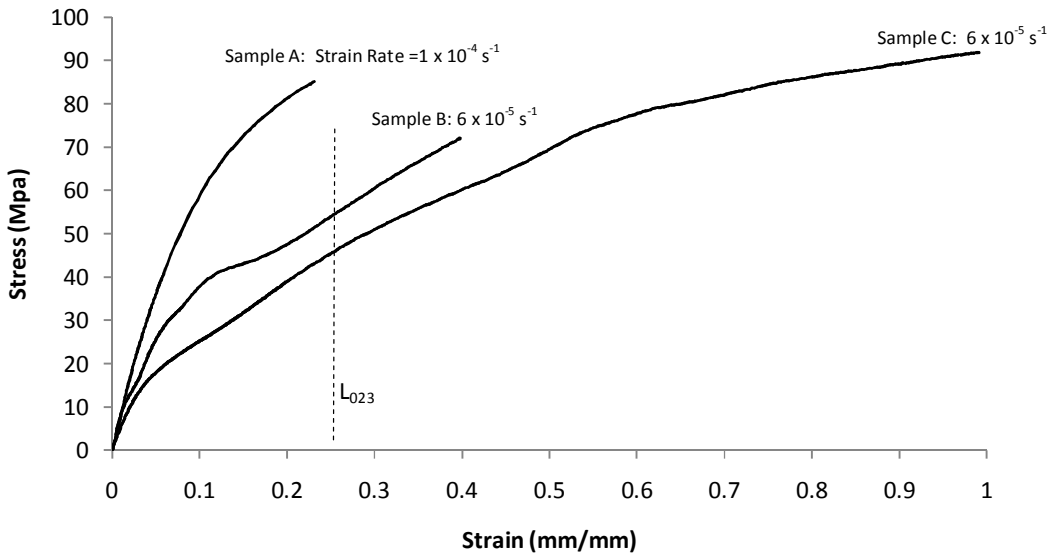

Figure 4.8 Stress and strain relationship at different strain and strain rate.

4.2.2 Effect of Strain Rate and Strain on Boronized Layer

Figure 4.9 depicted the microstructure after deformation process. The development of surface disintegration and cracking herein was learnt to be associated with the flow stress during forming. It is apparent in this image that at strain rate of 6 x 10^{-5} s^{-1} sample B has excellent compressibility and can be deformed without surface disintegration until strain of 0.4 mm/mm. Sample A with strain of 0.4 mm/mm and strain rate of 1 x 10^{-4} s^{-1}, shows surface disintegration in the form of micro-cracking propagated towards the core. Sample B bearing a lower flow stress than sample A justified this condition. In sample C, even as the strain rate is kept the same as with sample B, the surface disintegration can be observed due to higher strain applied. From the observation, it is important to identify the optimum condition to avoid surface disintegration. Strain rate control and the amount of strain applied are very critical to generate the best outcome.

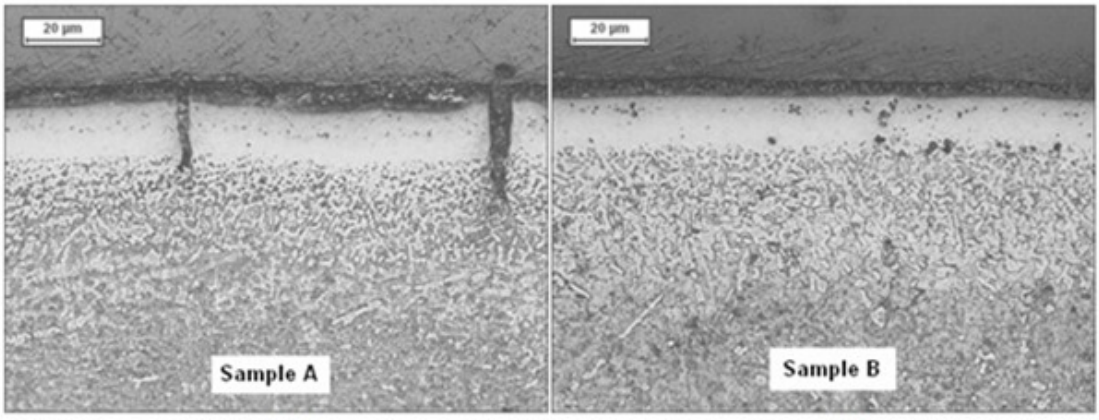

(a) (b)

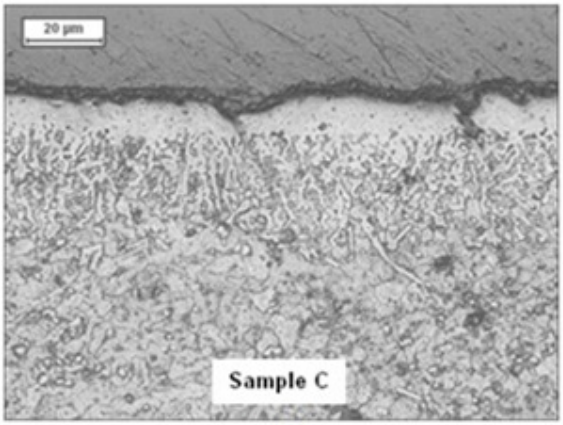

(c)

Figure 4.9 Cross sectional view of specimens after deformation (a) Strain rate = 1 x 10^{-4} s^{-1} and strain 0.4 mm/mm, (b) Strain rate = 6 x 10^{-5} s^{-1} and strain 0.4 mm/mm and (c) Strain rate = 6 x 10^{-5} s^{-1} and strain 1.0 mm/mm

CHAPTER 5

CONCLUSIONS

The focus of this study had been the formation of mini gear with superplastic deformation from thermo-mechanically treated boronized duplex stainless steel subjected to several characterization assessments to be finally tested against its determining parameters, i.e. strain and strain rate. The results are summarized as follows:

(a) Boronizing was successfully performed onto the duplex stainless steel (DSS) specimen producing boronized layer with surface hardness of 2253 HV and uniform boronized layer thickness of 40 μm.

(b) Surface integrity was found on the boronized layer deformed at 6×10^{-5} s^{-1} strain rate and 0.4 mm/mm strain. The boronized layer demonstrated failure to withstand the increased load when deformed at 1×10^{-4} s^{-1} strain rate. At 6×10^{-5} s^{-1} strain rate and 1.0 mm/mm strain, the surface disintegrity was associated to high strain factor.

(c) Surface disintegration in the form of micro-cracking propagated towards the core was found in Sample A. Sample B has excellent compressibility and can be deformed without surface disintegration until strain of 0.4 mm/mm. In sample C, micro-cracking propagated towards the core even as the strain rate is kept the same as with sample B due to higher strain applied. Strain rate control and the amount of strain applied are very critical to generate the best outcome.

CHAPTER 6

RECOMENDATIONS

Some suggestions to be considered in further developing this formation of mini gear with superplastic deformation on boronized duplex stainless steel technique as follows:

- To consider a new material for die set. Current H13 material used in this study tend to deformed after several compression processes under high temperature. Material such as Inconel should be considered in future development for this project.
- Further evaluation such as wear and corrosion resistance test on the mini gear formed should be carried out to measure the outcome of the specimen.
- Further study should focus on finding the optimum strain and strain rate parameter for specific and more accurate mini gear form.

REFERENCES

Ahmad, N.W., Jauhari, I., Azis, S.A.A., Azis, N.H.A. (2010). Surface properties and activation energy of superplastically carburized duplex stainless steel. *Material Chemistry and Physic.* **122 (2-3).** *454-458*

Allaoui, O., Bouaouadja, N. and Saindernan, G. (2006). Characterization of boronized layers on a XC38 steel. *Surface and Coatings Technology*. **201 (6).** *3475-3482*

Arieli, A. And Mukherjee, A.K. (1980). A model for the rate-controlling mechanism in superplasticity. *Materials Science and Engineering.* **45 (1).** *61-70*

Bartsch, K. and Leonhardt, A. (1999). Formation of boride layers on steel by d.c. plasma boriding and deposition process. *Surface and Coating Technology.* **116-119.** *386-390*

Béjar, M.A. and Moreno, E. (2006). Abrasive wear resistance of boronized carbon and low- alloy steels. *Journal of Materials Processing Technology.* **173.** *352-358*

Biddulph, R.H. (1997). Boronizing for erosion resistance. *Thin Solid Films.* **45 (2).** *341-347*

Cabrera, J.M., Mateo, A., Llanes, L., Prado, J.M., Anglada, M. (2003). Hot deformation of duplex stainless steels. *Journal of Materials Processing Technology.* **143-144.** *321-325*

Chandra, N. (2002). Constitutive behavoiur of superplastic materials. *International Journal of Non-Linear Mechanics.* **37.** *461-484*

Charles, J. and Vincent, B. (1997). Duplex stainless steels for chemical tankers. *Proceedings of Duplex Stainless Steel 97 - 5th World Conference.* Netherlands. *727-736.*
URL: http://www.stainless-steel-world.net/pdf/d97_018.pdf

Chokshi, A.H. (2005). Cavity nucleation and growth in superplasticity. *Materials Science and Engineering A.* **410-411.** *95-99*

Coiley, J.A. (1974). Technology of superplasticity. *Physic in Technology.* **5.** *86-90*

Davis, J. R. (2002). *Surface Hardening of Steels: Understanding the Basics.* Materials Park, OH, USA: ASM International

Dieter, G.E. (1986). *Mechanical Metallurgy.* 3rd edn. London: McGraw-Hill Inc.

Filep, E. and Farkas, S. (2005). Kinetics of plasma-assisted boriding. *Surface and Coatings Technology.* **199.** *1-6*

Friedman, P.A., Luckey, S.G. (2004). On the expanded usage of superplastic forming of aluminium sheet for automotive applications. *Material Science Forum.* **447-448.** *199-204*

Friedrich, H.E. and Winkler, P.J. (1991). Fundamental questions concerning the application of superplastic forming and superplastic forming/difussion bonding. In Hori, S., Tokizane, M. and Furushiro, N. (eds). *Superplasticity in Advance Materials. 601-610*

Genel, K., Ozbek, I. and Bindal, C. (2003). Kinetics of boriding of AISI W1 steel. *Materials Science and Engineering.* **A347.** *311-314*

Gifkins, R.C. (1976). Grain-boundry sliding and its accomodation during creep and superplasticity. *Metallurgical and Materials Transactions A*. **7.** *1225-1232*

Goeriot, P., Fillit, R., Thevenot, F., Driver, J.H. and Bruyas, H. (1982). The influence of alloying element additions on the boriding of steels. *Materials Science and Engineering.* **55 (1).** *9-91*

Goeriot, P., Thevenot, F. and Driver, J.H. (1981). Surface treatment of steels: Borudif, a new boriding process. *Thin Solid Films.* **78 (1).** *67-76*

Han, Y.S. and Hong, S.H. (1997). The effects of thermo-mechanical treatments on superplasticity of Fe-24Cr-7Ni-3Mo-0.14N duplex stainless steel. *Scripta Materialia.* **36.** *557-563*

Han, Y.S. and Hong, S.H. (1999). Microstructural changes during superplastic deformation of Fe-24Cr-7Ni-3Mo-0.14N duplex stainless steel. *Materials Science and Engineering*. **A266.** *276-284*

Hefti, L. (2004). Bonded components. *Materials science Forum.* **447-448.** *177-182*

Hertzberg, R.W. (1996). Deformation *and Fracture Mechanics of Engineering Materials,* 4th edn. New York: John Wiley & Sons.

Huang, J.C. and Chuang, T.H. (1999). Progress on superplasticity and superplastic forming in Taiwan during 1987-1997. *Materials Chemistry and Physics.* **57.** *195-206*

Jain, V. and Sundararajan, G. (2002). Influence of the pack thickness of the boronizing mixture on the boriding of steel. *Surface and Coatings Technology.* **149.** *21-26*

Jauhari, I., Ogiyama, H. and Tsukuda, H. (2002). Superplastic difussion bonding of duplex stainless steel. *Proceeding of 2nd World Engineering Congress.* Malaysia. *117-121*

Jauhari, I., Yusof, H.A.M., Saidan, R. (2011). Superplastic boronizing of duplex stainless steel under dual compression method. *Materials Science and Engineering A.* **528.** *8106– 8110*

Jiménez, J.A., Frommeyer, G., Carsí, M. and Ruano, O.A. (2001). Superplastic propperties of a δ/γ stainless steel. *Materials Science and Engineering A.* **307.** *134-142*

Keddam, M. and Chentouf, S.M. (2005). A diffusion model for describing the bilayer growth (FeB/Fe_2B) during the iron powder-pack boriding. *Applied Surface Science.* **252(2).** *393-399*

Langdon, T.G. (1970). Grain boundry sliding as a deformation mechanism during creep. *Phil. Mag.* **22.** *689-700*

Langdon, T.G. (1991). The Physic of superplastic deformation. *Materials Science and Engineering A.* **137.** *1-11*

Li, Z. and Guo, H. (2005). Application of superplastic forming and diffusion bonding in the aerospace industry. *Materials Science Forum.* **475-479.** *3037-3042*

Lutfullin, R.Y., Imayev, R.M., Kaibyshev, O.A., Hismatullin, F.N. and Imayev, V.M. (1995). Superplasticity and solid state bonding of the TiAl intermetallic compound with micro- and submicrocrystalline structure. *Scripta Metallurgica et Materialia.* **33(9).** *1445-1449*

Mabuchi, M. and Higashi, K. (1998). The processing, properties and applications of high strain rate superplastic materials. *Journal of the Menerals, Metals and Materials Society.* **50 (6).** *34-39*

Melendez, E., Campos, I., Rocha, E. and Barron, M.A. (1997). Structural and strength characterization of steels subjected to boriding thermomechanical process. *Materials Science and Engineering.* **A234-236.** *900-903*

Meric, C., Sahin, S. and Yilmaz, S.S. (2000). Investigation of the effect on boride layer powder particle size used in boronizing with solid boron-yielding substance. *Materials Research Bulletin.* **35.** *2165-2172*

Michael, P., Oliver, S., Thomas, G. (2007). Effect of intermetallic precipitations on the properties of duplex stainless steel. *Materials Characterization.* **58 (1).** *65-71*

Miyamoto, H., Mimaki, T., Hashimoto, S. (2001). Superplastic deformation of micro specimen of duplex stainless. *Materials Science Engineering.* **A319-321.** *779-783*

Mukherjee, A.L. (1971). The rate controlling mechanism in superplasticity. *Materials Science and Engineering.* **8 (2).** *83-89*

Nieh, T.G., Wadsworth, J., Sherby O. D. (1997). *Superplasticity in Metals and Ceramics*. New York: Cambridge University Press

Novaka, A.A., Sizov, I.G., Golubok, D.S., Kiseleva, T.Y. and Revokatov, P.O. (2004). Electron-beam boriding of low-carbon stel. *Journal of Alloys and Compounds.* **383.** *108-112*

Ogiyama, H., Shiraishi, T., Tsukuda, T. and Jauhari, I. (2001). *Journal Society of Material Science Japan.* **50**. *949* (in Japanese)

Ozbek, I., Konduk, B.A., Bindal, C., Zeytin, S., Ucisik, A.H. (2002). Characterization of borided AISI 316L stainless steel implant. *Vacuum.* **65.** *521-525*

Ozbek, I., Sen, S., Ipek, M., Bindal, C., Zeytin, S., Ucisik, A.H. (2004). A mechanical aspect of borides formed on the AISI 440C stainless steel. *Vacuum.* **73.** *643-648*

Prasad, Y.V.R.K. and Seshacharyulu, T. (1998). Processing map for hot working of titanium alloys. *Materials Science and Engineering A.* **243.** *82-88*

Ridley, N., Salehi, M.T. and Piling, J. (1992). Isostatic diffusion bonding of microduplex stainless steel. *Materials Science and Technology.* **8.** *791-795*

Sagradi, M., Pulino, D., Medrano, R.E. (1998). The effect of the microstructure on the superplasticity of a duplex stainless steel. *Acta Material.* **46 (11).** *3857-3862*

Sahin. S. and Meric, C. (2002). Investigation of the effect of boronizing on the cast irons. *Materials Research Bulletin.* **37 (5).** *971-979*

Selçuk, B., Ipek, R. and Karamiş, M.B. (2003). A study on friction and wear behaviour of carburized, carbonitrided and borided AISI 1020 and 5115 steels. *Journal of Materials Processing Technology.* **141.** *189-196*

Semiatin, S.L., Joseph, R.D., James, D.D., and Theodore, B.Z. (1998). Dies and die materials for hot forging. *Forming and Forging.* Ohio: ASM International.

Seshacharyulu, T., Medeiros, S.C., Frazier, W.G., and Prasad, Y.V.R.K. (2000). Hot working of commercial Ti-6Al-4V with an equiaxed α-β microstructure: materials modeling consideration. *Material Science and Engineering A.* **284.** *184-194*

Siegert, K. and Werle, T. (1994). *Combination of Superplastic Forming and Diffusion Bonding*. European Aluminium Association.
URL: http://www.eaa.net/eaa/education/TALAT/lectures/3805.pdf

Sinha, A.K. (1991). Boronizing, ASM Handbook, OH, USA. *Journal of Heat Treatment.* **4.** *437-447*

Superform Metal Limited (eds). (1988). *Superplastic Aluminium Forming.* United Kingdom: Gulliver Press Ltd.

Taktak, S. (2006). Tribological behaviour of borided bearing steels at eleveted temperatures. *Surface and Coatings Technology.* **201.** *2230-2239*

Tsuzaki, K., Xiaoxu, H. and Maki, T. (1996). Mechanism of dynamic continous recrystallizing during superplastic deformation in a microduplex stainless steel. *Acta Metallurgica.* **44 (11).** *4491-4499*

Tsuzuka, T., Takahashi, A. and Sakamoto, A. (1991). Application of superplastic forming for aerospace components. In Hori, S., Tokizane, M. and Furushiro, N. (eds). *Superplasticity in Advance Materials.* (p. 611-620)

Tuomi, A., Lofstrand, A., and Harju, M. (2000). Increased usage of duplex materials in manufacturing of pulping equipment. *Proceeding of Duplex America 2000 Conferece.* USA. *401-408*
URL: http://www.stainless-steel-world.net/duplex/pand.asp

Venkataraman, B. and Sundararajan, G. (1995). The high speed sliding wear behaviour of boronized medium carbon steel. *Surface and Coatings Technology.* **73.** *177-184*

Xing, H., Zhang, K., Qiao, Y. and Wang, Z.R. (1995). An advance superplastic sheet-forming machine contrilled by microcomputer. *Journal of Materials Processing Technology.* **55.** *43-47*

Xing, H.L., Wang, C.W., Zhang, K.F., Wang, Z.R. (2004). Recent Development In The Mechanics Of Superplasticity And Its Application. *Journal of Materials Processing Technology.* **151.** *196-202*

Xun, Y.W. and Tan. M.J. (2000). Applications of superplastic forming and diffusion bonding to hollow engine blades. *Journal of Materials Processing Technology.* **99.** *80-85*

Yapar, U., Basman, G., Arisoy, C.F., Yesilcubuk, S.A. and Sensen, M.K. (2004). Influence of boronizing on mechanical properties of EN-C35E steel. *Key Engineering Materials.* **264-268.** *629-632*

Yu, L.G., Chen, X.J., Khor, K.A. and Sundararajan, G. (2005). FeB/Fe2B phase transformation during SPS pack-boriding: Boride layer growth kinetics. *Acta Materialia.* ***53.*** *2361-2368*

Zainul, H. (2004). Optical Microscopy. *A 2-Day Short Course on Materials Analysis, Characterization and Evaluation.* University of Malaya, Kuala Lumpur, Malaysia.

Zelin, M.G. and Mukherjee, A.K. (1996). Geometrical aspects of superplastic flow. *Materials Science and Engineering A.* **208.** *210-225*

INTERNET REFERENCE

URL: 1) http://www.mse.mtu.edu/~drjohn/sp/deform/

URL: 2) http://www.surfaceengineering.com/Products-CVD.htm

URL: 3) http://www.bortec.de/Frame1_englisch.html

URL: 4) http://www.asminternational.org/asmenterprise?APD/SearchAPD.aspx

URL: 5) http://en.wikipedia.org/wiki/X-ray_scattering_techniques

URL: 6) http://www.otago.ac.nz/geology/facilities/minerologypetrology/index.html

URL: 7) http://sirius.mtm.kuleuven.be/Research/Equipment/fiches/xl40-fic.html